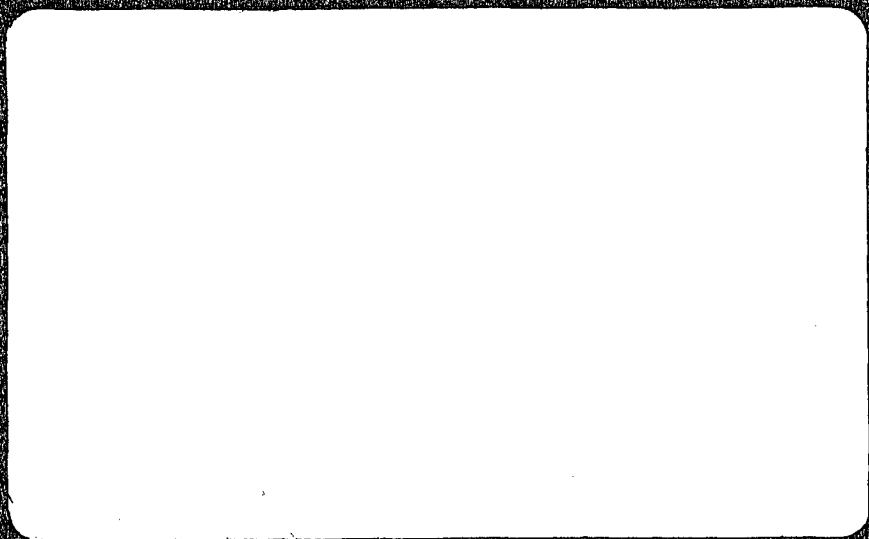


YEIP
04-071
2004



AURORA GEOSCIENCES LTD.
GEOLOGICAL AND GEOPHYSICAL CONSULTANTS
YELLOWKNIFE, CANADA
WHITEHORSE, Y.T. CANADA

**INDUCED POLARIZATION
AND VLF SURVEY AT
THE DRAGON LAKE PROPERTY,
YUKON TERRITORY**

DRAG 1-4 YB67142-45
DRAG 5-6 YB96313-14
DRAG 7-8 YB96608-09
DRAG 13-14 YC09170-81
DRAG 25-44 YC18115-34

for: **BOOTLEG EXPLORATION INC.**
Suite 200, 16 - 11th Avenue South
Cranbrook, B.C., V1C 2P1

by: Dave Hildes, Ph. D.
Aurora Geosciences Ltd.
108 Gold Road
Whitehorse, Yukon, Y1A 2W3

Surveyed: June 21 – July 11
Location: 62° 36' N 131° 31' W
NTS: 105 J/12, J/11
Mining District: Whitehorse
Date: Dec 2004

YUKON ENERGY, MINES
& RESOURCES LIBRARY
PO BOX 2703
WHITEHORSE, YUKON Y1A 2C6

YMIP 04-071

SUMMARY

Induced polarization / resistivity (IP) and VLF-EM surveys were conducted on the Dragon Lake Property for Eagle Plains Resources Ltd to locate additional gold mineralization on the property. The IP survey was to delineate the calc-silicate horizon bearing the auriferous sulphides. The VLF survey was to identify structural features which appear to concentrate gold values.

A total of 7.1 line-km were cut and chained to survey 6.3 line-km of IP / resistivity using a dipole-dipole array with 25 m dipole spacing, reading from the 1st to the 6th separation. The data were interpreted by employing automated computer inversion to generate 2D models of the chargeability and resistivity distribution along each line. These results were in turn contoured to generate three dimensional models of chargeability and resistivity. 3.4 line-km of VLF data were also collected.

The survey identified a zone of elevated chargeability that is 300 metres wide (300 S to 0 N) and extends from line 200 W to line 300 E. The zone is open to the east. Several showings with elevated gold values are coincident with this zone. Previous drill testing did not intersect the highest chargeabilities. One small VLF anomaly may indicate a NNW structure within this zone. Drilling the chargeable highs within this zone is recommended.

A thin (10-50 m), shallow, chargeable zone was also identified close to the baseline (0 N) from L300 W to L100 E. This feature correlates well with elevated gold soil geochemistry. Previous drill testing did not intersect areas of highest chargeability. A strong VLF anomaly may indicate a NNW structure within this anomaly. Trenching and drilling are recommended to test this feature.

LIST OF FIGURES

Figure 1. Property location 2

Figure 2. Claim location 3

Figure 3. Grid map Back Pocket

Figure 4. Regional geology 16

Figure 5. Stacked resistivity models Back Pocket

Figure 6. Stacked chargeability models Back Pocket

Figure 7. Plan view of resistivity and chargeability models 19

Figure 8. ESE view of resistivity and chargeability models 20

Figure 9. WNW view of resistivity and chargeability models 21

Figure 10. Chargeability model on 1999 diamond drill hole traces 22

Figure 11. Stacked VLF-EM profiles 25

1.0 INTRODUCTION

Aurora Geosciences Ltd. was retained by Bootleg Exploration Inc. to perform VLF and induced polarization / resistivity (IP) surveys at the Dragon Lake Property. The gold mineralization is largely confined to a pyrrhotite-pyrite-chalcopyrite sulphide horizon in a calc-silicate succession, striking roughly 110 degrees. Within the sulphide horizon, the gold appears to be concentrated along NNW striking structures showing replacement style mineralization. The VLF survey was designed to identify these structures, while the IP survey was designed to image the sulphide horizon.

A total of 7.1 line-km were cut (baseline and IP) and 6.3 line-km surveyed with IP. 3.4 line-km of VLF were surveyed along uncut lines. The work was done between June 21 and July 11, 2004. This report describes the survey, data processing and results and contains an interpretation of the data and recommendations for further work.

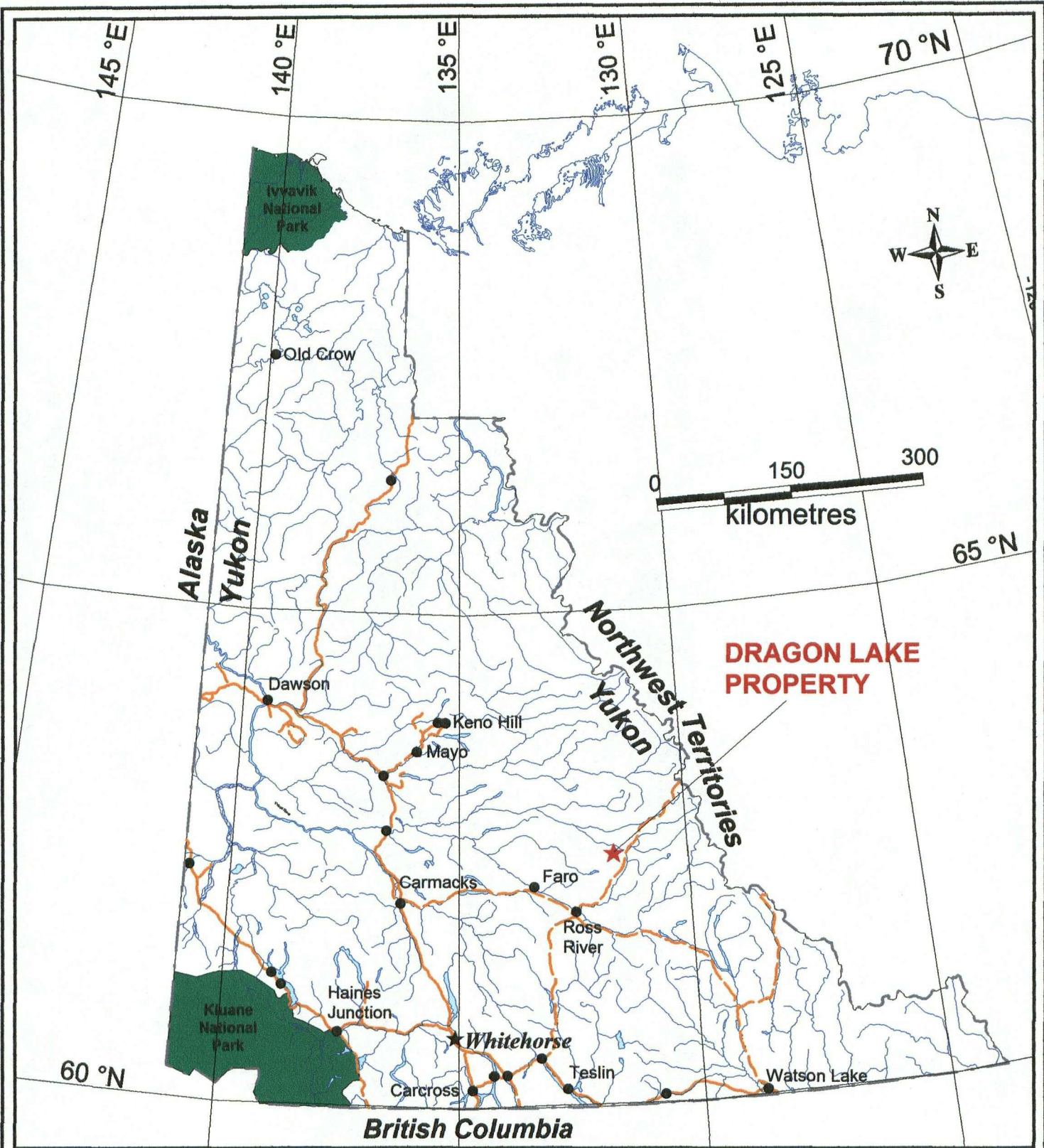
2.0 LOCATION AND ACCESS

The Dragon Lake Property is located in the Whitehorse Mining District, approximately 85 km northeast of the town of Ross River, centered at 61° 36' N, 131° 31' W on NTS map sheet 105 J/12 and J/11 (Figure 1). It comprises 40 Quartz claims in the Whitehorse mining district (Figure 2), detailed below. The property is situated along the south shore of Dragon Lake, 10 km from the North Canal road. Access was by boat from the government boat launch on the North Canal road. A good campsite was found just north of the grid on line 0E.

Claim Name	Grant #	Expiration Date
DRAG1 – DRAG4	YB67142 – YB67145	2007 / 06 / 28
DRAG5 – DRAG6	YB96313 – YB96314	2007 / 09 / 20
DRAG7 – DRAG8	YB96608 – YB96609	2007 / 09 / 30
DRAG13 – DRAG24	YC09170 – YC09181	2005 / 12 / 07
DRAG25 – DRAG44	YC18115 – YC18134	2005 / 12 / 07

3.0 GRID

The survey grid is shown in Figure 3 (back pocket); it is in an area of moderate topography, with one narrow, deep creek gully along line 300W. Grid cutting and installation was performed by the Aurora Geosciences crew prior to the IP survey.



**BOOTLEG EXPLORATION INC
 DRAGON LAKE PROPERTY
 LOCATION MAP**

Figure 1

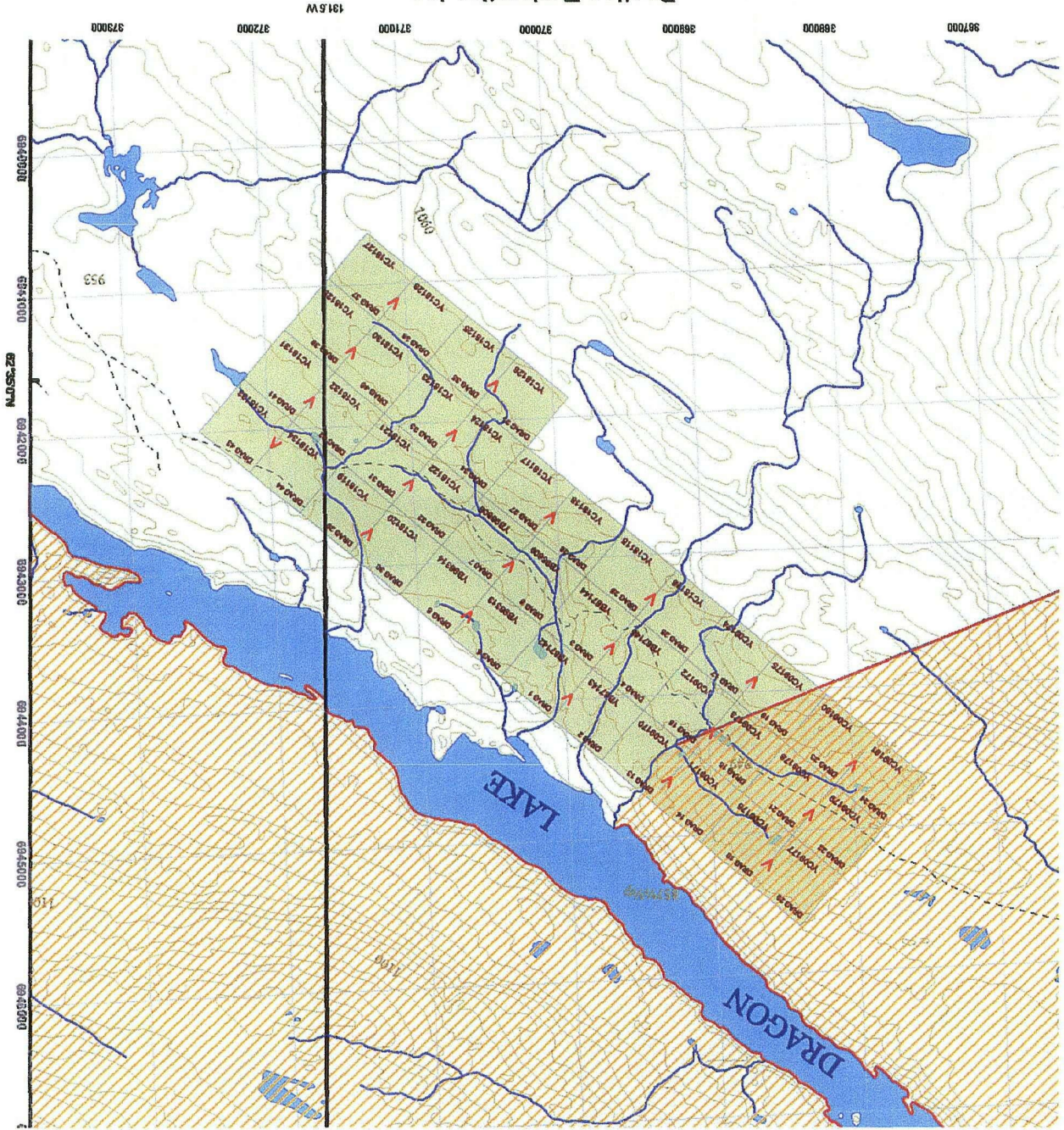
December 13, 2004

Aurora Geosciences Ltd.

NTS: 105 J12
Date: Mar 2004
Proj: UTM Zone 9N Mining District: Whitehorse
Datum: NAD83
Job: BEI-04-003-YT

Figure 2
Claim Map

Bootleg Exploration Inc.



Recent forest fires have left predominantly buck brush, poplar and heavy wind-throw of larger trees which resulted in low line-cutting production. An 800 m base line trending 110 degrees was cut and nine lines were turned and cut 300 m grid-north and 400 m grid-south. The lines were chained and picketed at 25 m intervals with no slope corrections. Line-ends and baseline-intersections were recorded using non-differential GPS and these measurements were used to register the grid to geographic coordinates (UTM Zone 9N, NAD83).

Four VLF lines, trending 60 degrees, were put in by hip-chain and compass. These lines were flagged and not cut. Line-ends and several midpoints were recorded using non-differential GPS and these measurements were used to register the grid to geographic coordinates (UTM Zone 9N, NAD83).

4.0 PERSONNEL AND EQUIPMENT

The survey was conducted by the following personnel:

<u>Crew chief / geophysicist :</u>	Dave Hildes, Ph. D.
<u>Technician:</u>	Warren Kapaniuk
<u>Helper:</u>	Anna Crawford
<u>Helper:</u>	Qamar Khan

The crew was equipped with the following instruments and general equipment:

<u>IP Transmitter:</u>	GDD TX-II 1.8 KW digital IP transmitter Honda 5KVA gas generator
<u>IP Receiver:</u>	IRIS ELREC 6 digital 6-channel IP receiver.
<u>Other IP equipment</u>	6 km 18 gauge wire in good repair. Breast reels and speedy winders Stainless steel electrodes VHF radios 25 m 6-channel receiver cables Tools and repair equipment
<u>VLF</u>	Geonics EM-16 VLF receiver

Camp: 1 - 4 man summer camp (2 - 12'x14' tents, kitchen gear, generator, SAT phone) and boat

Line cutting: 3 - chain saws
1 - line cutting crew kit (hip chains, chains, GPS receivers, prisms etc.) including pickets, tags & flagging

Data processing: Pentium-4, 2.67GHz laptop
Geosoft IP package

5.0 SURVEY SPECIFICATIONS

The survey was conducted according to the following specifications:

Array: Dipole-dipole

Dipole spacing: 25 m

Separations read: n=1 to 6

Tx mode / signal: Standard time domain signal (0.125 Hz, 50% duty cycle, reversing polarity)

Receiver sampling: Semi-logarithmic sampling of the decay curve in 10 windows, stacked minimum 15 times.

Parameters read: M_t - total chargeability (mV/V)
 R_o - apparent resistivity (Ohm m)
 M_1 to M_{10} - 10 channel samples of decay curve
 V_p - Primary voltage
 Sp - spontaneous potential
E - error in chargeability (mV/V)

Noise: Standard deviation of the chargeability was kept to 5 mV/V or less wherever possible. If this was not possible, readings were repeated several times to determine their repeatability.

VLF: Station spacing of 25 m on 4 cross-lines using the Jim Creek, Washington (NLK) station, azimuth 153.

Facing direction All VLF measurements taken facing grid west.

Other: Line-ends and baseline-crossings were measured with non-differential GPS and IP station-to-station slopes were recorded with a hand-held clinometer to provide topography for the inversion. All coordinates are UTM Zone 9N, NAD83.

6.0 SURVEY NOTES

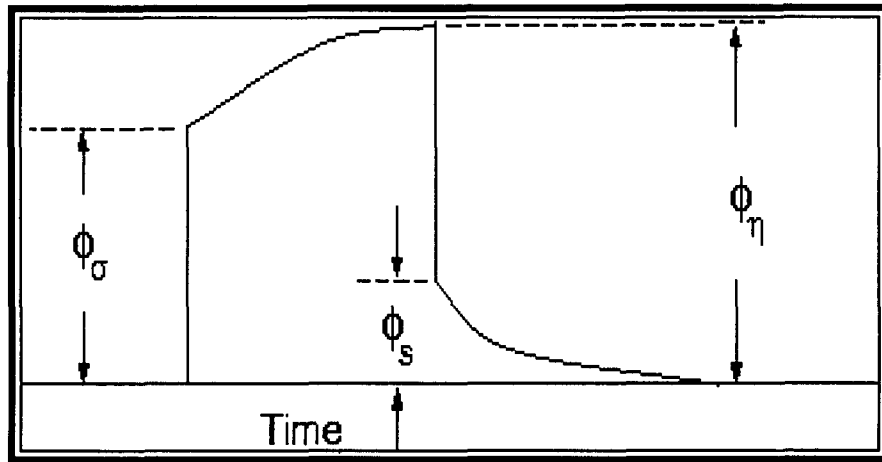
The survey log in Appendix B describes detailed survey operations including production. The crew mobilized to the property on June 21st and June 22nd by truck from Whitehorse to Dragon Lake and then by boat from the government launch at the North Canal road to the property. Line cutting proceeded from June 22nd to June 29th, with the VLF survey performed on June 26th. The IP survey commenced June 29th. Late in the afternoon of June 30th, the IP transmitter broke-down and a spare was sent from Whitehorse, which was picked up at the boat launch early on July 1st. On the afternoon of July 3rd, the replacement transmitter failed and as no replacement was available, the crew demobilized to Whitehorse. On July 8th, the crew re-mobilized from Whitehorse and set up camp at the North Canal road. Two more days of work (commuting by boat) completed the project and the crew demobilized on July 11th. Data quality was generally good, except along rocky outcrops on ridge-tops where poor electrode contacts due to lack of soil resulted in noisy data.

7.0 IP INTERPRETATION METHOD

The data were interpreted using the DCIP2D package developed by the University of British Columbia Geophysical Inversion Facility. The inversion algorithm is described in detail by Oldenburg and Li (1994). A brief description of key features of the algorithm follows.

The IP effect can be described in macroscopic terms. If a time domain signal is put into the ground, as soon as the current is turned on, the voltage immediately rises to a level (ϕ_{σ}) and thereafter continues to rise to a higher level (ϕ_{η}). At current shutoff, the voltage immediately falls to a level (ϕ_s) and then slowly decays to zero along a curve similar to that between ϕ_{σ} and ϕ_{η} . Apparent chargeability is defined as the "extra" voltage observed:

$$\eta_a = \frac{\phi_{\eta} - \phi_{\sigma}}{\phi_{\eta}} = \frac{\phi_s}{\phi_{\eta}}$$



IP response curve (UBC DCIP2D documentation, 1998)

The observed DC potentials ϕ_σ are defined by the vector form of Ohms Law:

$$\nabla \cdot (\sigma \nabla \phi_s) = -I \delta(r - r_s)$$

where $\mathbf{r}-\mathbf{r}_s$ is the vector to the measurement point, I is the current and σ is the conductivity structure of the earth - the unknown quantity in the geophysical problem. The chargeability can be modeled by replacing the conductivity by an equivalent apparent conductivity controlled by the chargeability:

$$\sigma_\eta = \sigma(1 - \eta)$$

Modeling the IP effect then involves running two conductivity models - one with σ and one with σ_η .

The unknown quantity is the distribution of conductivities in the earth. The software models the earth conductivity structure as a series of rectangular cells of varying size and aspect ratio. The grid is finest (most detailed) near the measurement points and much coarser at locations beside or at depth beneath the measurement points. The padding cells are necessary to avoid having edge effects appear in the model. The size and dimensions of the models in no way compensates for the basic limitations on depth penetration and resolution inherent in the IP/resistivity survey. Thus the effective depth of penetration (0.5 to 1.0 times the maximum dipole separation) is the limit to which the models should be relied upon to accurately reflect true earth conductivities and chargeabilities.

The program calculates the potential across the finite element network using a starting model. Appropriate boundary conditions are applied when calculating the potentials across the network. These include the condition that all current flow is normal to the cell boundaries and voltages are continuous across the boundaries. The sensitivity of the model to changing the parameters in any cell is calculated as is the misfit between the model results and the actual observed potentials / chargeabilities. The model is then adjusted using the calculated sensitivities of the response to changes in the conductivity of individual cells.

There is no unique solution or model which fits any set of IP / resistivity data. A best-fit model is one which (1) fits the data within the error of the survey and (2) invokes the minimum required degree of complexity to fit the data. For a set of **N** measurements, a global misfit can be defined as:

$$\Psi_d = \sum_{i=1}^N (W_i (r_i - r_i^{obs}))^2$$

where W_i is the weighting factor for the i^{th} measurement (r^{obs}) and r_i is the model response for this measurement. The weighting factor is usually the inverse of the error so that a measurement with high error has a low weighting and vice versa. In a system with random noise, the target misfit is **N**. The algorithm reduces Ψ_d by repeatedly adjusting the conductivities to improve the fit until the global misfit equals the target misfit. At this point, the model fits the data to within the error of the survey.

The second requirement of a successful solution is that the complexity of the final model be minimized. IP measurements are inherent averages, deriving resistivity and chargeabilities from large volumes of the subsurface. It is possible to over-fit data, deriving solutions which over-minimize misfit but which invoke models with detail beyond the resolving power of the measuring arrays. The problem is ill-posed and inherently ambiguous in that an infinite number of models may satisfy the global misfit equals target misfit criterion. If both a simple and complex solution can adequately replicate the field data within the bounds of measurement error, the simple solution is to be preferred.

Starting with a reference model m_0 and weighting functions for x and z (w_x , w_z), define the complexity of the model as Ψ_m where:

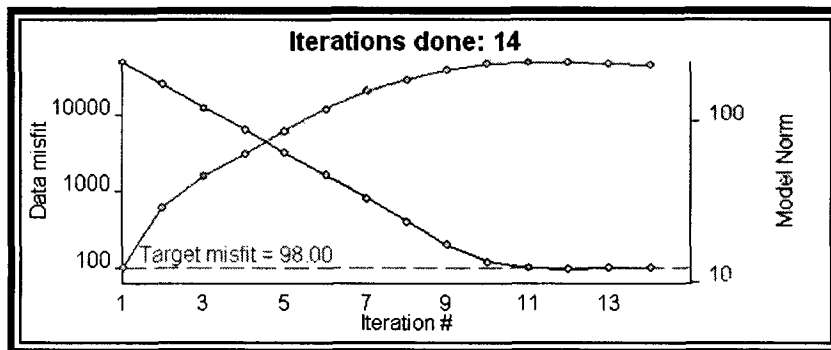
$$\psi_m(m, m_0) = \alpha_s \int \int w_s(x, z) (m - m_0)^2 dx dz + \int \int \left\{ \alpha_x w_x(x, z) \left(\frac{\partial(m - m_0)}{\partial x} \right)^2 + \alpha_z w_z(x, z) \left(\frac{\partial(m - m_0)}{\partial z} \right)^2 \right\} dx dz$$

where α_x , α_z and α_s define the relative weight of the model in x, z and fineness. Increasing any of these values increases the importance of that dimension in the final solution. For example, to weight the final solutions towards vertical structures, α_z would be weighted several times more than α_x . To force the model to generate fewer small scale structures, α_s is increased.

The final criteria for a successful solution can then be expressed as:

1. Minimize Ψ_m
2. Subject to the constraint that $\Psi_d = N$ (or very close to it).

To evaluate a solution, the reader should examine not only the final values but the path the program followed to reach these values. An example of typical convergence curves is shown below:



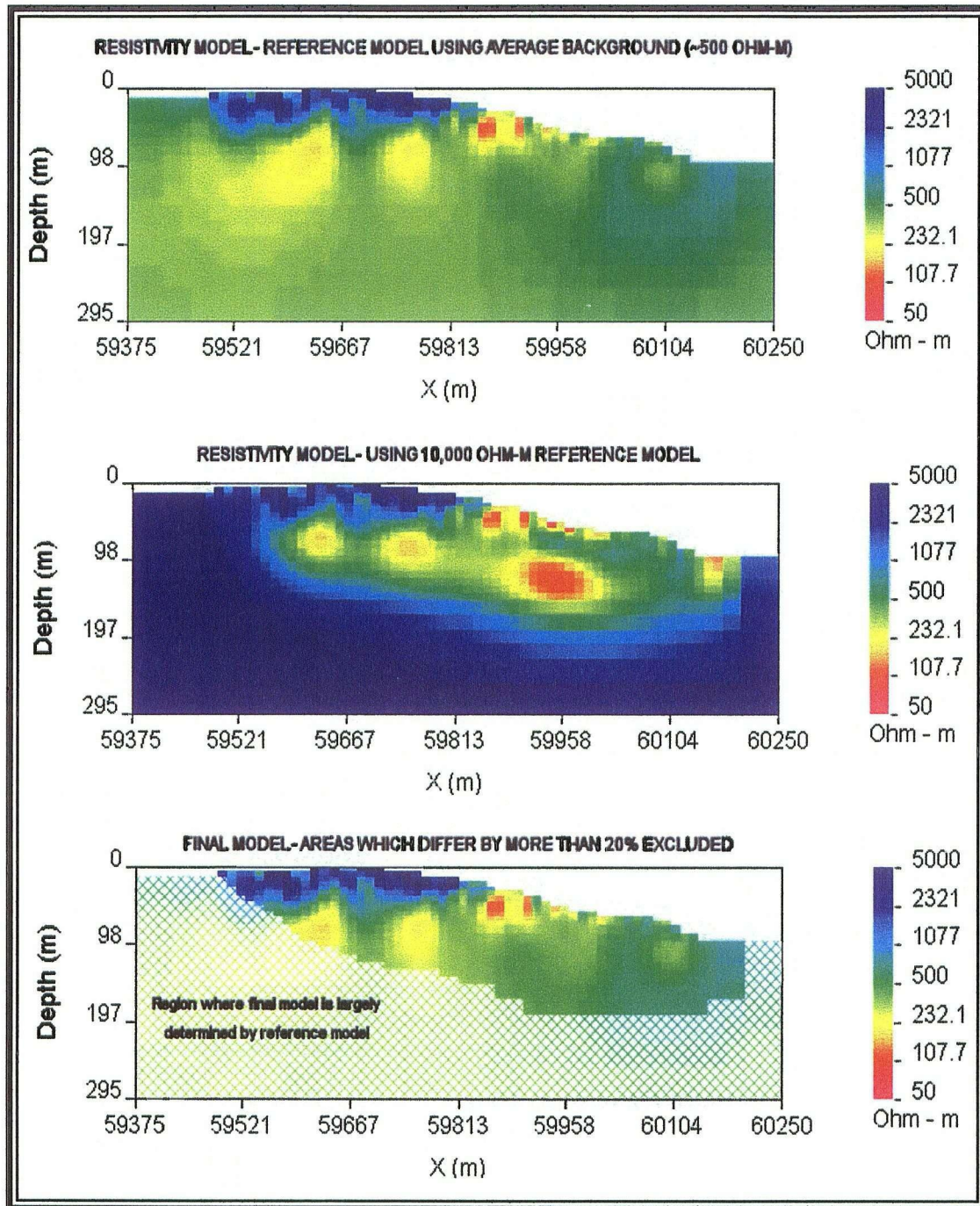
Typical convergence curves - DC inversion

The black line traces the value of Ψ_d with each iteration and in a good inversion, this will converge to the target misfit (N). The orange curve traces the convergence behavior of Ψ_m . This curve normally starts at a very small value because the reference model is usually set to the initial model and the initial and reference models are very simple. As the inversion proceeds, the solution model becomes increasingly complex as it is adjusted to meet the target misfit. After reaching target misfit, minor adjustments

are made to reduce the complexity of the model and the Ψ_m curve stabilizes at some high value.

The field observations often have significant poorly quantified errors and the complexity of the background conductivity response may be such that it is impossible to reduce Ψ_d to N. Instead, Ψ_d can be scaled proportionately by a "chi-factor" ranging up or down from 1.0 (no scaling). Setting a large chi-factor loosens the control that goodness-of-fit exerts on the solution and generally directs the program to use very simple models which tend to smooth out the conductivities and fails to accurately model the fine details in resistivity or chargeability known to exist in the ground. Setting a chi-factor which is too low may prevent convergence to an acceptable solution. Generally, chi is left at 1.0.

A final feature of note in the inversion is the use of initial and reference conductivity and chargeability models in the inversion process. As noted above, the relation for Ψ_m requires a reference model (m_0) against which solutions are compared. This can be an actual 2D model constructed from known geology or a estimate of half space conductivity or chargeability. In addition, the modeling process will start from an initial model which has the same general form. In general, an average half space conductivity and chargeability based on the field values is the best model to start from and this is the default model for both inversions if none other is specified. This will ensure that Ψ_m converges to a value which is not too large. The initial and reference models can be used to estimate the depth of investigation. If two inversions are performed with very different reference models, there will be regions in the final models which will be the same in both inversion and peripheral regions where the final models will resemble the reference models. An example is shown below:



Depth of investigation determined from inversion results using different initial and reference models.

8.0 DATA PROCESSING

The following procedures were used to prepare and invert the induced polarization and resistivity data:

- 1. Data review.* The IP data were reviewed and edited prior to preparing pseudosections and preparing the data sets for inversion. During data collection, data with error greater than 5 mV/V were repeated, multiple times if data were not repeatable. Outliers were rejected, then repeat readings were averaged to leave only a single reading at each station and separation. If multiple readings were not repeatable, no data for that station and separation were processed further.
- 2. Pseudosection plotting.* Pseudosections of the apparent resistivity, chargeability and error in chargeability were prepared from the final edited data using the Geosoft IP package. Consistent scales (logarithmic 107-1275 Ohm-m for apparent resistivity and linear 6-63 mV/V for apparent chargeability) were used. Pseudosection plots are in Appendix E, found in the back pocket of this report.
- 3. Data formatting.* The apparent chargeability, resistivity (in normalized Voltage over Current) and topographic data were formatted for entry into the UBC inversion program.
- 4. Resistivity modelling.* For each line, errors in the apparent conductance were assigned to the data. There is no means of directly quantifying these errors because neither the transmitter nor receiver record the error in the current or voltage. Errors were assumed to be $0.0002 + 5\%$ S/m. Following error assignment, the data were inverted. A deep mesh was constructed to adequately incorporate the topography on the grid. Default initial and reference models were used, based on an average of the apparent resistivity. After the default run, the data were inverted a second time using initial and reference models of 10,000 Ohm-m (a much higher value than the average in the survey area). The purpose of this second run was to generate a model with a background resistivity greatly different than the average values used in the default run. After the second run, the two models were compared and regions which showed more than 10% discrepancy were blanked out from the default run. In these blanked out regions, the final model is not sensitive to the field data and there is no reliable subsurface information.
- 5. Chargeability modelling.* For each datum, the observed standard deviation of chargeability was used as a measure of error for apparent chargeability. To avoid zero errors, a minimum of 0.5 mV/V was added to each error

measurement. The IP data were first inverted using default values, with the same mesh as the resistivity modelling, using the default recovered resistivity model. After the first run, the data were inverted a second time using initial and reference models which incorporated background chargeabilities of 300 mV/V (a much higher value than the average in the survey area). The two models were then compared and regions which showed more than 10% discrepancy were blanked out in the final models. In these blanked out regions, the final model is not sensitive to the field data and there is no reliable subsurface information.

On lines 000 E the target misfit could not be achieved and the condition $\Psi_d = N$ was relaxed to ensure convergence. Nevertheless, the observed data and recovered data match sufficiently well to use the inversion results in further processing steps.

6. Image extraction. After the modelling was complete, data ranges were compiled and overall data scales were assigned for both the resistivity and chargeability models. A logarithmic scale covering a range of 50 to 5,000 Ohm-m was used as a standard scale for all resistivity models. A scale of 0 to 80 mV/V was used in all chargeability model sections. Final images were generated with the inversion software and converted to JPEGs which appear in Appendix D. Stacked sections of the models were compiled in Figures 5 and 6.

7. 3D model generation. The inversion results for each lines were converted to UTM coordinates and elevation using proprietary software and plotted with Rockworks 3D imaging software. The gridding algorithm used to create the 3D model is a inverse-distance, directionally weighted method to account for higher data density along the line direction. The ground surface (from digital topography) is used as an upper bounding surface. After the data are gridded, residuals are modelled and the final model is tweaked to better honour the control points. A clipping filter was applied to reject artifacts outside the grid. Lastly a smoothing filter was applied. Slices of the model along drill traces were extracted from the pre-smoothed model. Numerous views of the 3D model are found in Figures 7 through 10.

8. Digital archive. The final IP data, digital copies of the pseudosections, inversion images and 3D images were written to CD-ROM.

The following procedures were used to prepare the VLF data:

- 1. Data entry and registration.* The VLF data were transferred from field notes to a database and registered to UTM coordinates using proprietary software.
- 2. Profile plotting.* Stacked inphase and quadrature profiles were plotted for the

four lines. Data was interpreted and subsurface conductors identified (see Figure 11.)

3. *Digital archive.* The final database and a digital copy of the stacked profiles were written to CD-ROM.

9.0 DATA PRODUCTS

The following data files are appended to the digital version of this report

Dragon2004_IPdata.xyz	ASCII file with final IP / resistivity data. Readings with unacceptable errors and which did not repeat have been deleted.
Dragon2004_IPdata.gdb	Final IP / resistivity data in geosoft IP database. Readings with unacceptable errors and which did not repeat have been deleted.
Dragon2004_IPgps.txt	ASCII file with line-ends and baseline-crossings GPS locations. All coordinates are in UTM zone 9N, NAD83.
Dragon2004_VLFdata.xyz	ASCII file with inphase and quadrature VLF data. UTM coordinates (Zone 9N, NAD83) are included in this data base.
Dragon2004_VLFdata.gdb	Inphase and quadrature VLF data in geosoft database. UTM coordinates (Zone 9N, NAD83) are included in this data base.
Dragon2004_VLFgps.txt	ASCII file with line-ends and line-midpoints GPS locations. All coordinates are in UTM zone 9N, NAD83.

The following images are appended to the digital version of this report

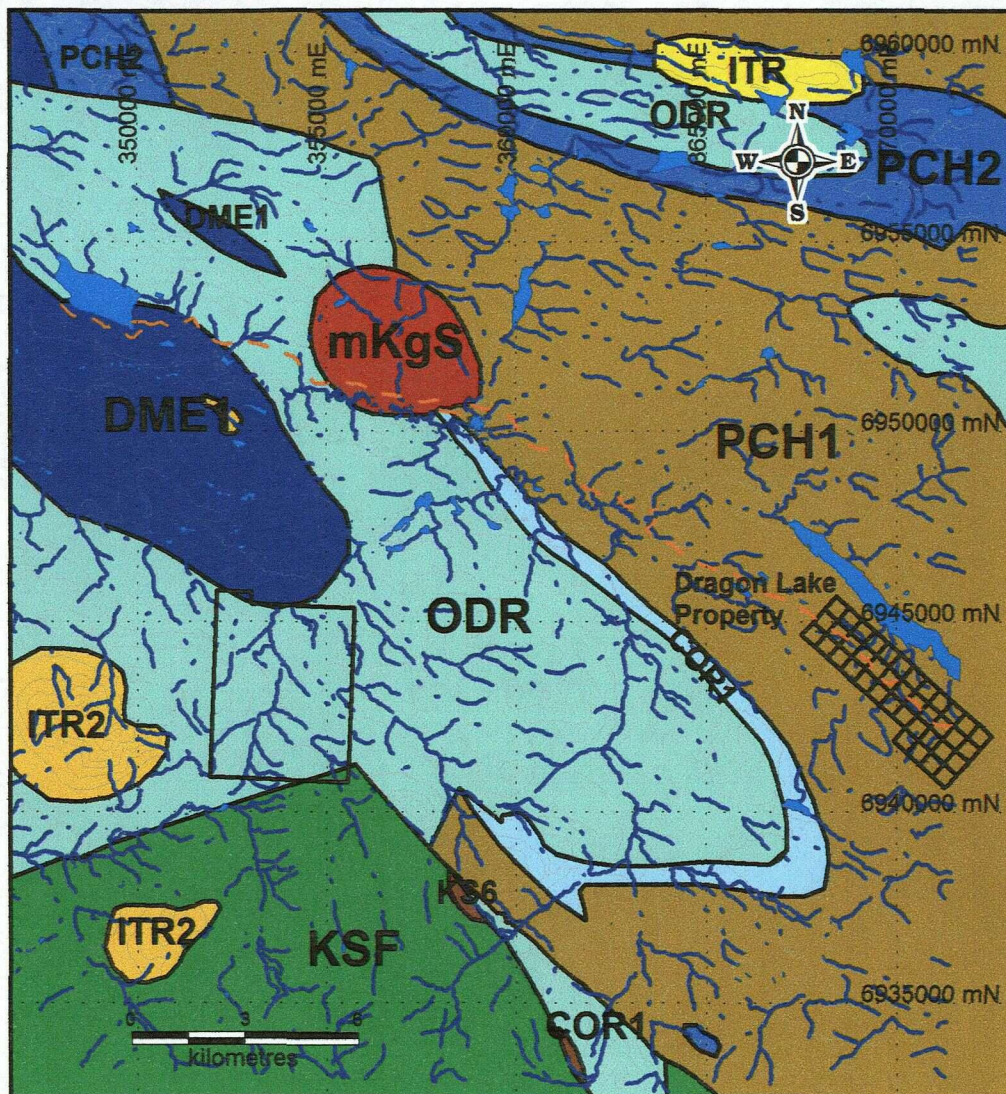
L300E.pdf	Pseudosections of apparent chargeability, apparent resistivity and error in apparent chargeability. All plots are at a scale of 1:2500. Paper plots of these pseudosections are in Appendix E, back pocket of the report.
L200E.pdf	
L100E.pdf	
L000E.pdf	
L100W.pdf	
L200W.pdf	
L300W.df	
L400Wpdf	
L500W.pdf	
L300E - IP model.jpg	Inversion results for all lines. The "model" images have the recovered model with the depth of investigation (described above) and the convergence curves to assess the quality of the inversion. The "pseudo" images have the both observed data and the calculated data from the recovered model. Paper copies of these plots are in Appendix D.
L300E - IP pseudo.jpg	
L300E - res model.jpg	
L300E - res pseudo.jpg	
...	
L500W - IP model.jpg	
L500W - IP pseudo.jpg	
L500W - res model.jpg	
L500W - res pseudo.jpg	

10.0 GEOLOGICAL SETTING

The Dragon Lake Property is underlain by sedimentary rocks of the Selwyn Basin that have been intruded by rocks of the Selwyn Suite intrusives. The oldest layered rocks in the area are the Upper Proterozoic Hyland Group. These are overlain by the Upper Cambrian and Ordovician Rabbitkettle Formation; followed by the Ordovician to Lower Devonian Road River Group; the Devonian to Mississippian Earn Group; the Lower Cretaceous Sharp Mountain Formation; the mid-Cretaceous South Fork Volcanics; and Lower Tertiary Ross Formation (Figure 4).

The Hyland Group is divided into two packages in the Dragon Lake area. The upper package consists of thin to thick bedded, brown to pale green shale with fine to coarse grained quartz-rich sandstone, grit, and quartz-pebble conglomerate, minor argillaceous limestone, phyllite, quartzo-feldspathic and micaceous psammite, gritty psammite and minor marble (PCH1) (Gordey, 1999). The lower package consists of grey weathering, dark grey to grey white, thin to thick bedded, very fine crystalline limestone, locally sandy, calc-silicate and marble (PCH2).

The Rabbitkettle Formation consists of thin bedded, wavy banded, silty limestone and grey lustrous calcareous phyllite, limestone intraclast breccia and conglomerate with



LEGEND

- ITR** Lower Tertiary (mostly Eocene)
Ross Formation - basalt and rhyolite
- ITR2** - rhyolite flows, tuff, ash, breccia and small stocks
- KSF** mid-Cretaceous
South Fork Volcanics - biotite-quartz-hornblende-feldspar crystal tuff.
- KS6** Lower Cretaceous
Sharp Mountain Formation - chert, sandstone and conglomerate.
- DME1** Devonian to Mississippian
Earn Group - slate, arenite, wacke, conglomerate, siltstone, barite
- ODR** Ordovician to Lower Devonian
Road River Group - shale, chert and siltstone
- COR1** Upper Cambrian and Ordovician
Rabbitkettle Formation - limestone, phyllite, breccia, siltstone and shale
- PCH1** Upper Proterozoic to Lower Cambrian
Hyland Group - shale, sandstone, conglomerate, limestone and phyllite
- PCH2** - limestone, calc-silicate marble.
- mKgS** mid-Cretaceous
Selwyn Suite - K-feldspar-biotite-quartz monzonite and granodiorite.

NAD 83 UTM, zone 9
1:200,000

Figure 4
NTS 105J/12 Whitehorse Mining District

December, 2004

AURORA GEOSCIENCES LTD

massive to laminated, grey quartzose siltstone and chert and rare black slate with local mafic flows, breccia and tuff (COR1). The Road River Group consists of black shale and chert overlain by orange siltstone or buff, platy limestone (ODR). The Earn Group is comprised of thin bedded, laminated slate with thin to thickly interbedded fine to medium grained nodular and bedded barite with rare limestone (DME1).

The younger, overlying rocks are the Sharp Mountain Formation, which is comprised of dark grey weathering massive to poorly bedded chert sandstone and chert pebble conglomerate (KS6). It is overlain by South Fork Volcanics, which are dark brown weathering, locally columnar jointed, massive, densely welded biotite-quartz-hornblende-feldspar crystal tuff (KSF). These are capped by the Ross Formation which occurs as rhyolite flows, tuffs, ash-flow tuffs and breccias with small stocks of white weathering, flow banded, quartz-sanidine porphyry to granite porphyry (ITR2) and undivided, mixed bimodal basalt and rhyolite (ITR) in the northern part of the map sheet.

Intrusive rocks in the area are part of the Selwyn Suite, which is comprised of resistant, blocky, fine to coarse grained equigranular to porphyritic (K-feldspar) biotite-quartz monzonite, granodiorite and minor quartz diorite and syenite.

The property geology consists of units of quartzite and limestone, marble, calc-silicate and skarn rocks generally striking 120 degrees and dipping 45 to 65 degrees northeast. The calc-silicate and skarn units host sulphide (predominantly pyrrhotite) mineralization with auriferous concentration along NNW structures.

11.0 RESULTS

11.1 IP / RESISTIVITY

Plots of all pseudosections are found in Appendix E (back pocket of this report). Appendix D contains a full suite of inversion results with convergence curves, modelled and observed data. Stacked model sections of resistivity and IP are in Figures 5 and 6 (back pocket). The red bars on Figures 5 and 6 show the elevated gold soil response (northern anomaly only). Assayed samples in anomaly A are in blue, anomaly B in red and anomaly C in green. The interpreted VLF conductors are also shown in Figures 5 and 6. Figures 7 through 9 are views of the 3D model constructed from inversion results with 20 mV/V chargeability contoured in red and 300 Ohm-m resistivity contoured in blue. Figure 10 shows extracts of the 3D model along the 1999 diamond drill traces.

Below is a line by line detailed review of the IP / resistivity results followed by a data review classified by anomaly. The stacked resistivity and chargeability models (Figures 5 and 6) and Appendix D are useful reference while reading the line by line

anomaly descriptions.

Line by line review:

Line 300E - Elevated chargeabilities (30-40 mV/V) throughout the section, except at the extreme north. Very chargeable 25 m anomaly centered at 325 S is coincident with a resistivity low (100 Ohm-m). Mineralized calc-silicate quartzite and skarn samples (BDR-26 and BDR-28) with 401 and 598 ppb Au were taken approximately 30 m east of the line. Resistivity in the rest of the section (200-500 Ohm-m) is not well correlated to the chargeability.

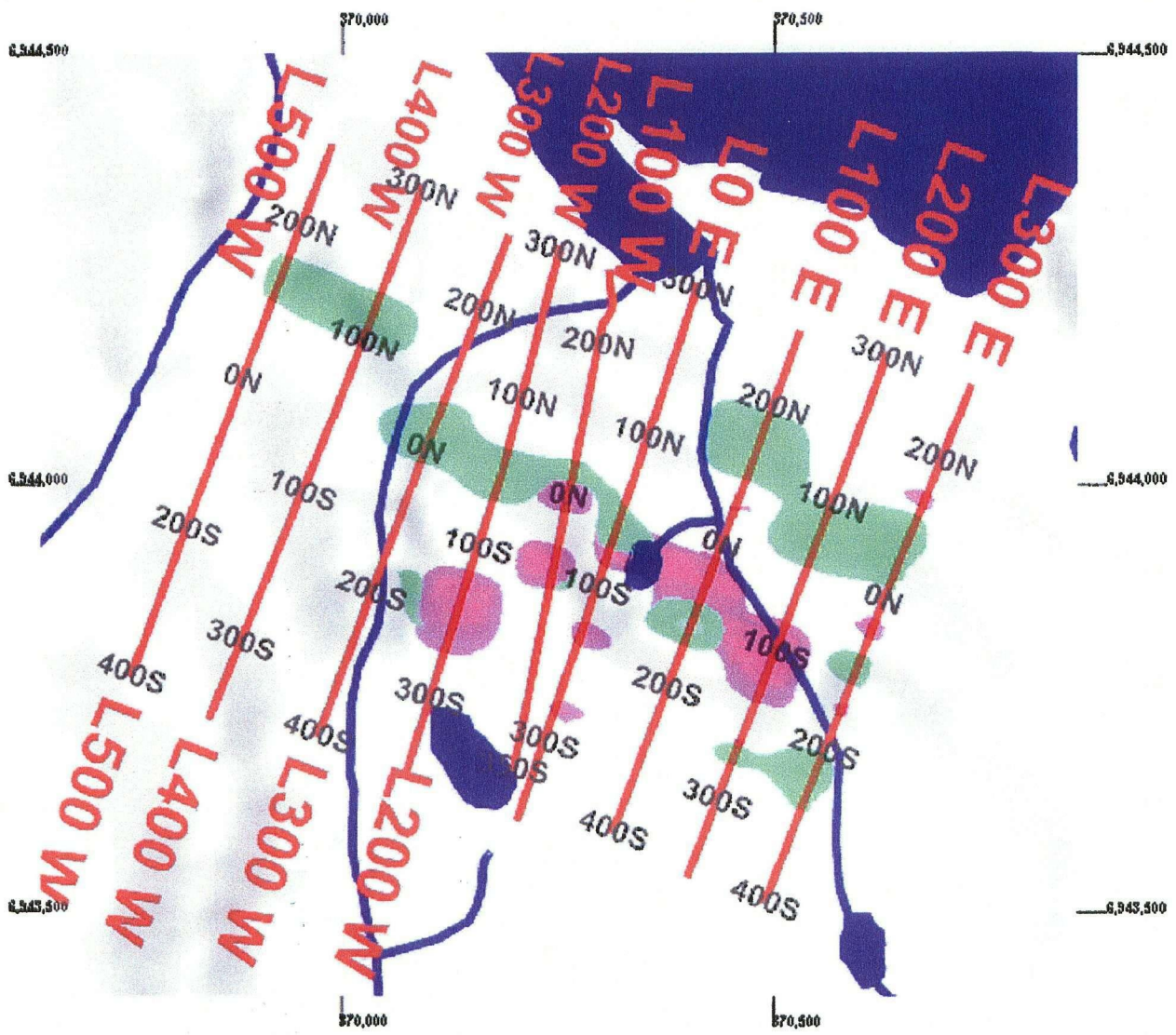
Line 200E - Elevated chargeabilities (40 mV/V) south of 50 S, extending to depth and a shallower 200 m anomaly centered at 50 N. There is a very chargeable point anomaly at 270 N with a calc-silicate quartzite sample BDR-21 (273 ppb Au) immediately south (and 50 m west). BDR-3 (5619 ppb Au) is at 50 S, 20 m west of the line. The northern end of the line is conductive (200 Ohm-m). There is no correlation between the resistivity and chargeability. Diamond drill holes D99-02 and D99-03 were collared at approximately 100 S.

Line 100E - A broad 200 m chargeable zone centered at 150 S. The southern end of this anomaly has a > 60 mV/V area, 60 m in length at 200 S, coincident with a conductivities of 50-100 Ohm-m. Another deep conductive zone of 100 Ohm-m, is at 90 N with no associated chargeability. Elevated gold soil geochemical values are found immediately north of a modest shallow chargeable zone on the baseline.

Line 000E - Three very chargeable zones (> 65 mV/V) are recovered in the southern portion of the model. A vertical structure at 275 S; a 60 m, north-dipping anomaly centered at 225 S; and a surface, point anomaly at 125 S. None are associated with resistivity lows. Showings T3 at 30 E, 130 S and T5 at 45 E, 160 S ran 19-400 ppb Au and 289-475 Au respectively. A fourth chargeable zone at 50 N lies within a 150 m surficial conductive zone (100 Ohm-m) centered at 25 N, coincident with the Au soil sample anomaly. Drill hole D99-01 collar is approximately 25 m east of station 100 N.

Line 100W - South of the baseline is a broad zone of elevated chargeability (40 mV/V). Within this are: a 50 m, north-dipping, 55 mV/V zone centered at 275 S; a 25 m, 65+ mV/V zone at 110 S; a shallow, thin 65 mV/V anomaly immediately north of the baseline. The latter two are within moderately (300 Ohm-m) conductive zones. Immediately north of the thin chargeable anomaly at the baseline is the gold soil geochemical anomaly

Line 200W - South of station 0 N is a broad anomaly of elevated (40 mV/V) chargeability with a 50 m, 60 mV/V area at 200 S and a 25 m, 50 mV/V zone at 25 S. The chargeable zones are immediately above 50-100 Ohm-m conductors. Showing T9



Bootleg Exploration Inc.

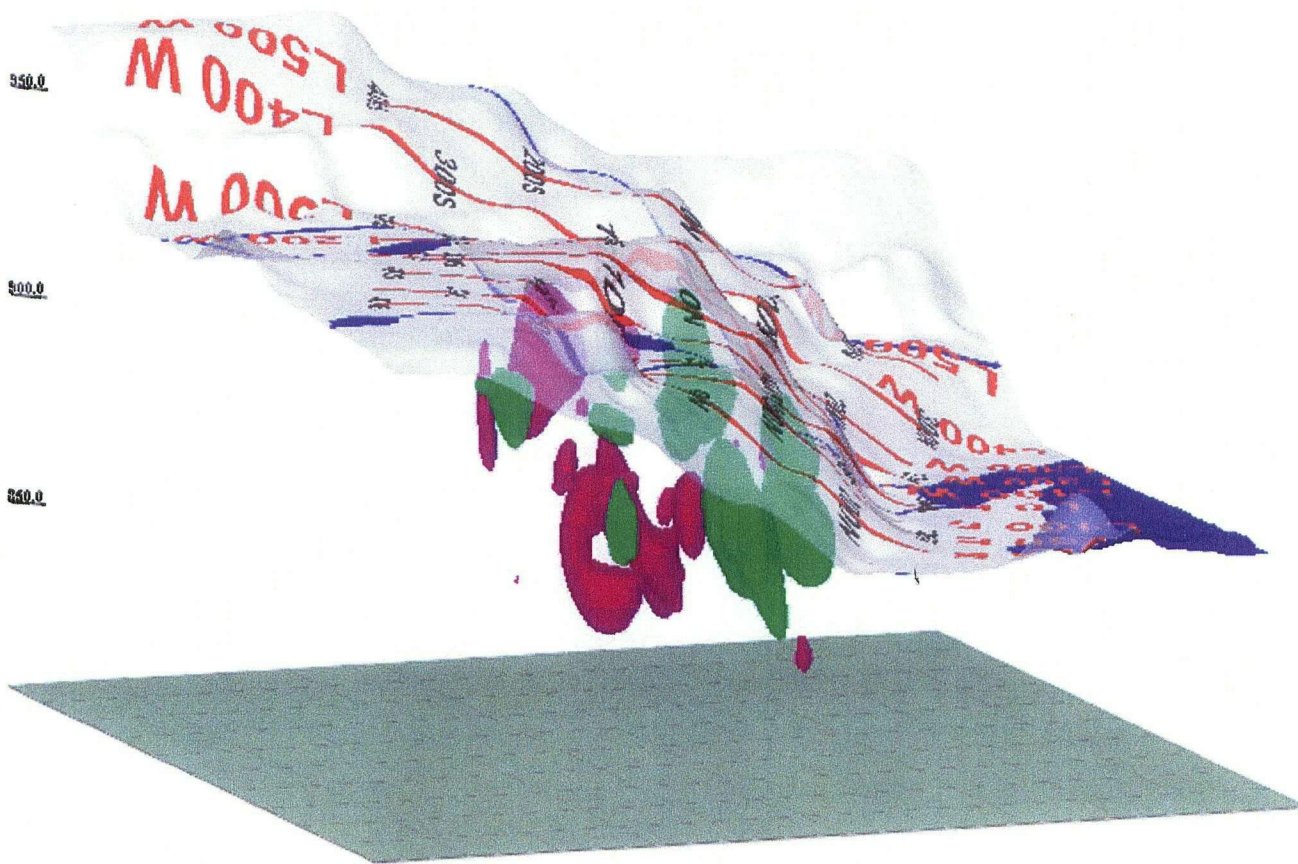
**Plan Map of Resistivity and Chargeability Models
Figure 7**

Green contour is 300 Ohm-m
Purple contour is 20 mV/V

NTS: 105 J/12
Proj: UTM Zone 9N
Date Surveyed: June / July 2004

Datum: NAD83
Mining District: Whitehorse
Job: BEI-04-003-YT

Aurora Geosciences Ltd.



Bootleg Exploration Inc.

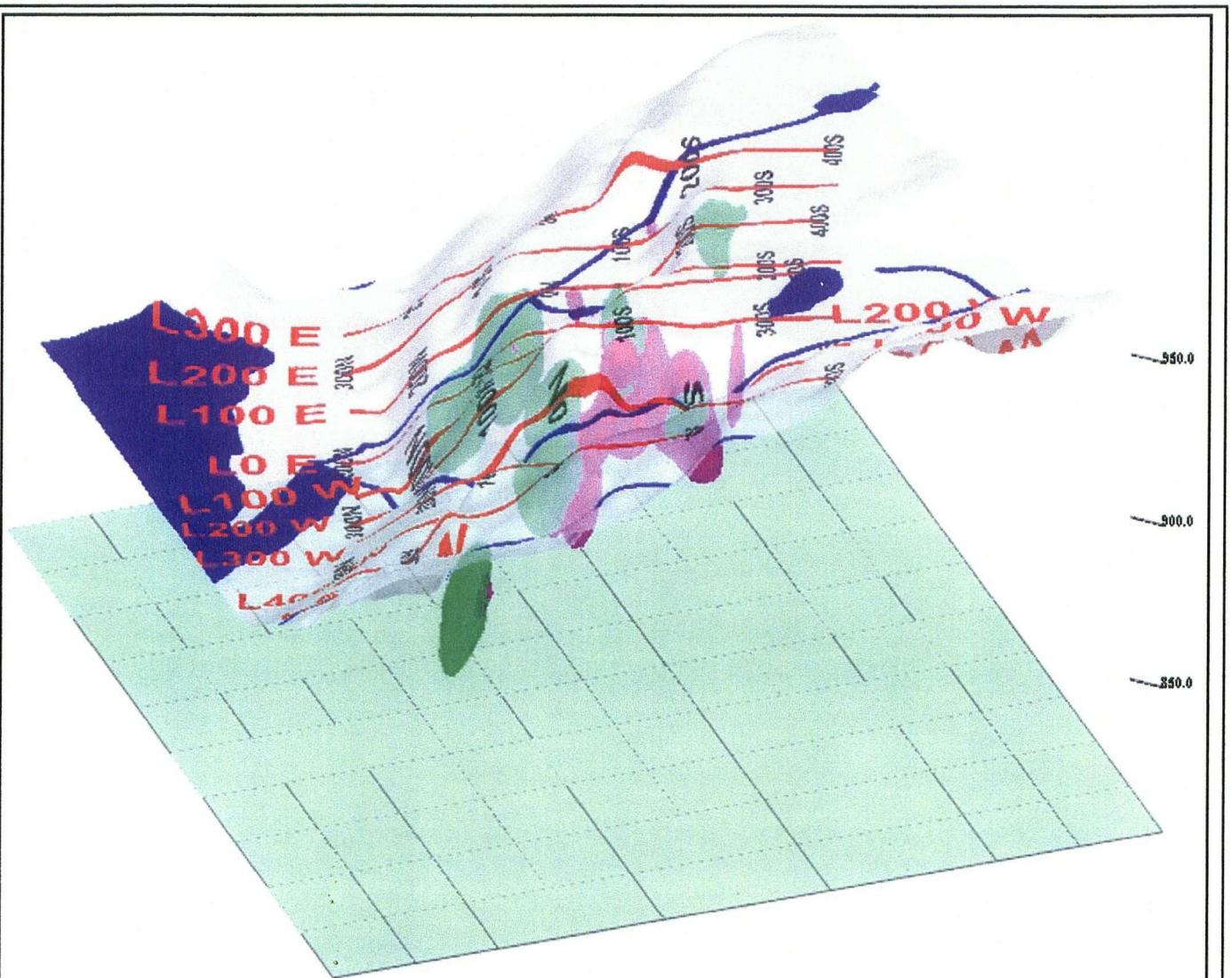
**ESE View of Resistivity and Chargeability Models
Figure 8**

Green contour is 300 Ohm-m
Purple contour is 20 mV/V
Vertical exaggeration = 4

NTS: 105 J/12
Proj: UTM Zone 9N
Date Surveyed: June / July 2004

Datum: NAD83
Mining District: Whitehorse
Job: BEI-04-003-YT

Aurora Geosciences Ltd.



Bootleg Exploration Inc.

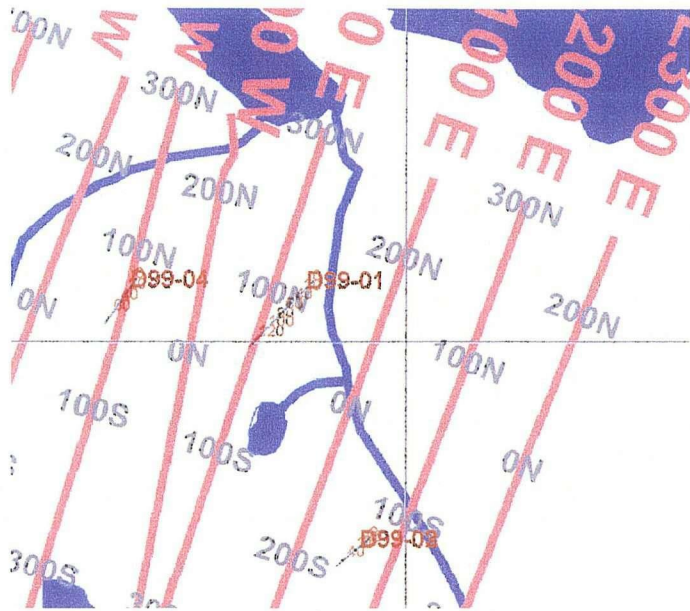
**WNW View of Resistivity and Chargeability Models
Figure 9**

Green contour is 300 Ohm-m
 Purple contour is 20 mV/V
 Vertical Exaggeration = 4

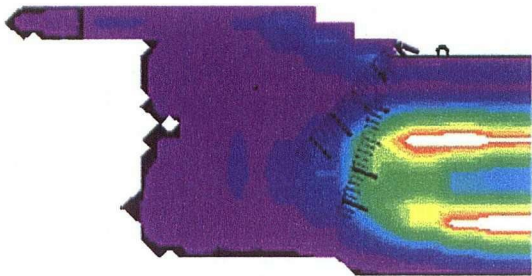
NTS: 105 J/12
 Proj: UTM Zone 9N
 Date Surveyed: June / July 2004

Datum: NAD83
 Mining District: Whitehorse
 Job: BEI-04-003-YT

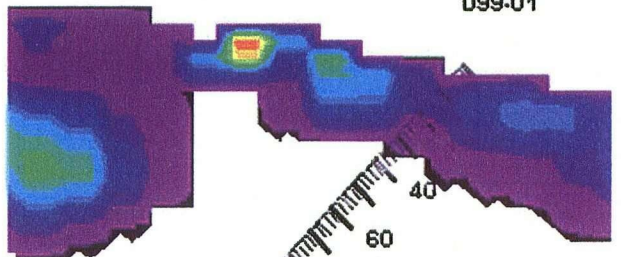
Aurora Geosciences Ltd.



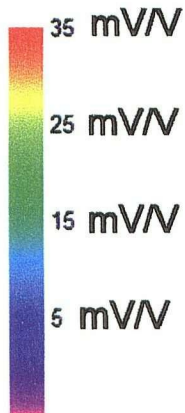
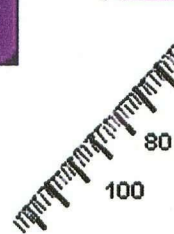
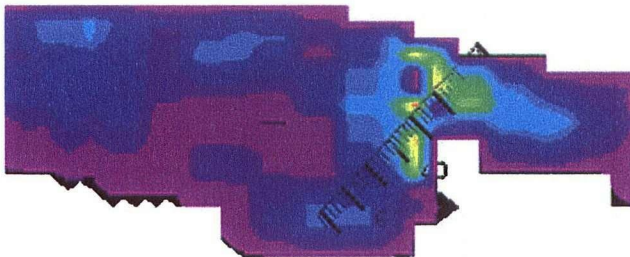
D99-03



D99-01



D99-04



Bootleg Exploration Inc.

Dragon Lake Property
 1999 Diamond Drill Holes
 with 3D Chargeability model
 Figure 10

Projection: Local grid
 Date Surveyed: June/July 2004

Mining District: Whitehorse
 Job: BEI-04-003-YT

Aurora Geosciences Ltd.

(446-1688 ppb Au) and the strong gold soil values are over the IP anomaly at 25S. Drill hole D99-04 was collared at approximately station 90 N.

Line 300W - Moderate chargeability (30-40 mV/V) anomalies (a 100 m anomaly centered at 25 S and 35 m anomaly at 215 S) sit on or above 50 Ohm-m resistivity lows. The soil geochemical Au anomaly is coincident with the geophysical anomaly at 25 S. Showing T12 at 340 W, 180 S is proximal to the anomaly at 215 S and ran 138-2296 ppb Au. Bad electrode contacts on the rocky outcrop around the baseline resulted in poor data quality in this region.

Line 400W - Moderate chargeability highs (30 - 40 mV/V) at 100 N, 225 S and 325 S are well correlated with resistivity lows. Showing T12 at 340 W, 180 S is proximal to the anomaly at 225 S and ran 138-2296 ppb Au and there are elevated gold soil responses over this feature. Showing T14 at 400 W, 30 N is proximal to the geophysical anomaly at 100 N and ran 111-1156 ppb Au. Bad electrode contacts on the rocky outcrop south of the baseline resulted in poor data quality in this region.

Line 500W - Modest chargeability highs (20 - 30 mV/V) at 100 N and 250 S are well correlated with resistivity lows.

Review by geophysical anomaly

In addition to the stacked resistivity and chargeability models (Figures 5 and 6), the 3D model views in Figures 7 through 9 show some of the features discussed below. Figure 7 is a plan map of the resistivity model (contoured at 300 Ohm-m in green) and the chargeability model (contoured at 20 mV/V in purple). Figures 8 and 9 have identical contours but are views from ESE (110 azimuth, 10 degrees above horizontal) and WNW (290 azimuth, 30 degrees above horizontal) respectively. Both Figures 8 and 9 have a vertical exaggeration of 4. Figure 10 consists of planar extracts of the 3D, unsmoothed, chargeability model along 1999 diamond drill hole traces.

Anomaly A - There is a 300 m wide zone (300 S to 0 N), from L200W and open to the east with chargeabilities greater than 40 mV/V. Within this zone, there are smaller pockets forming an arcuate band with further elevated chargeabilities (60-80 mV/V) at 325 S on L300 E; 275 S on L200 E; 200 S on L100 E; 275 S, 225 S and 125 S on L000 E; 275 S and 110 S on L100 W; 200 S on L 200 W. In general, the anomaly dips to the north. The resistivity varies within this zone and there is poor correlation between the resistivity and chargeability. Several showings and samples with elevated gold assays are found within this geophysical anomaly (all values in ppb Au): BDR-26 @ 401; BDR-28 @ 598; BDR-21 @ 273; BDR-3 @ 5619; T3 @ 19-400; T5 @ 289-475. Two holes (D99-02 and D99-03) have been drilled into this anomaly from the same collar location, neither of them targeting nor intersecting high chargeabilities (see Figure 10).

Anomaly B - A thin chargeable anomaly (50 m), becoming broader to the west, has a strike length of 400 m (from L100 E to L300 W), weaving around the baseline. Anomaly B intersects the IP lines at L100E @ 0 N; L000E @ 50 N; L100W @ 0 N; L200W @ 25 S; L300W @ 25 S. A possible diffuse anomaly could extend the strike length to the east. Because of the thin width, it is difficult to resolve in the 3D model and is more easily viewed on Figures 5 and 6. The anomaly tends to be conductive, either coincident with the chargeability or immediately below it. It is well correlated with the elevated gold soil geochemistry. On L100W and L100E, the soil anomaly is shifted slightly north (downslope). Trench T9, with high anomalous gold values is also within this zone. Two holes (D99-01 and D99-04) have been drilled into this anomaly, neither placement targeting nor intersecting the high chargeability areas (see Figure 10).

Anomaly C - Northern and southern branches of this coincident low-resistivity and moderate-chargeability anomaly on lines 500 W (@ 250 S and 100 N) and 400 W (at 300 S, 225 S and 100 N) may coalesce at L300W and represent a deeper extension of anomaly B. Showing T12 with 138-2296 ppb Au is proximal to the southern branch while T14 with 111-1156 ppb Au is close to the northern branch.

Anomaly D - In the northeast portion of the grid is a resistivity low with no associated chargeability. This unit dips to the north.

11.2 VLF-EM

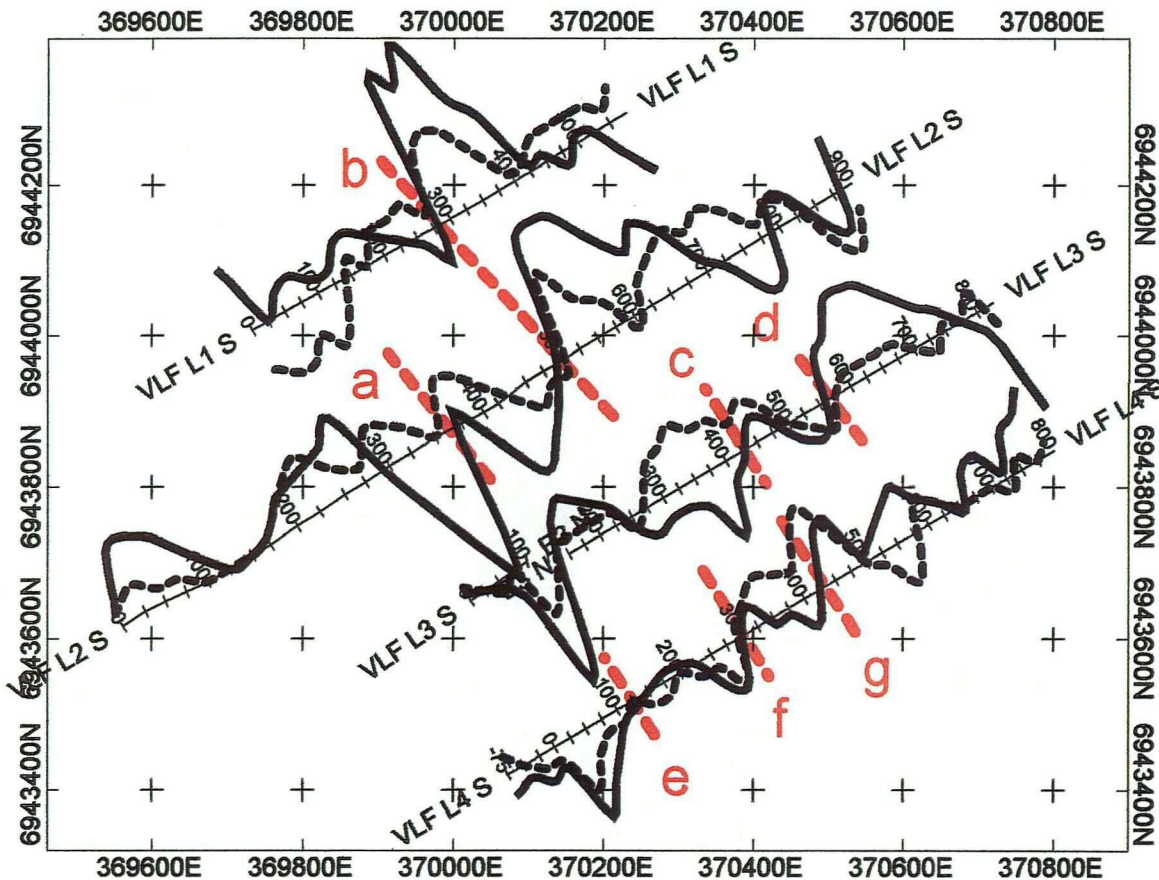
The VLF survey was designed to identify NNW structures along which the gold appears to be enriched. Figure 11 contains stacked profiles of the VLF inphase and quadrature responses with conductors identified in red. These are also shown on the stacked resistivity and chargeability models (Figures 5 and 6).

The largest VLF response and most robust interpreted conductor is labelled *b* on Figure 11, extending across VLF L1S and VLF L2S. This anomaly occurs on L400W at 35 N, L300W at 25 S and L200W at 75 S.

Smaller crossovers result in interpreted conductors labelled *c*, *d*, *e* and *f*. Anomaly *c* occurs on L100E at 125 S, anomaly *d* occurs on L200E at 0 N, and anomaly *f* occurs on L100E at 300 S and L200E at 375 S. Anomaly *e* is outside the IP grid.

Offset crossovers are labelled *a* and *g*. Anomaly *a* occurs at L300W at 230 S and anomaly *g* occurs at L200E at 200 S and L300E at 300 S.

The crossover at the west end of VLF L3 S is attributed to conductive lake bottom sediments.



LEGEND VLF-EM

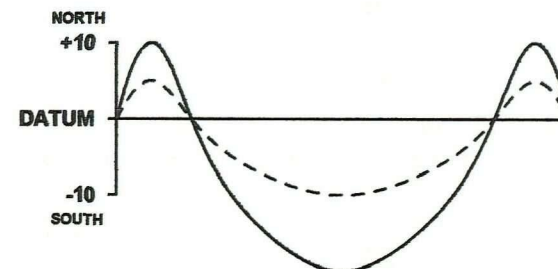
STATION : NLK (Jim Creek)

INSTRUMENT : Geonics EM-16

PROFILE SCALE : 1 cm = 10%

IN PHASE : _____

QUADRATURE : - - - - -



IN-PHASE DATUM : 0%

QUADRATURE DATUM : 0%

FACING DIRECTION : GRID WEST

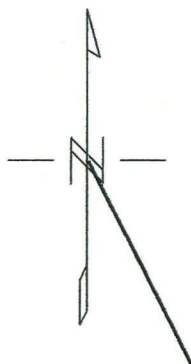
OPERATORS : DH, AC

DATA FILE : DragonVLF.gdb

STATION SEPARATION : 25 m

LINE-KM SURVEYED THIS SHEET : 3.36 km

 Interpreted conductor



NLK Jim Creek Wa (azimuth = 153)



Bootleg Exploration Inc.

**Dragon Lake Property, VLF-EM Survey
NLK (Jim Creek Washington) - Stacked Profiles
Figure 11**

NTS: 105 J/12

Projection: UTM Zone 9N

Date Surveyed: June/July 2004

Datum: NAD83

Mining District: Whitehorse

Job: BEI-04-003-TY

Aurora Geosciences Ltd.

12.0 INTERPRETATION & DISCUSSION

Some caution must be exercised in the geographic registration of previous work, which contains some errors. There are discrepancies for showing locations of at least 65 m between two maps in the 1999 diamond drill report. There are also discrepancies between the UTM coordinates and grid coordinates in the drill hole logs. Under the assumption that the errors are isolated rather than systematic, showing locations and drill collars have been plotted on the figures based on the 1999 diamond drill report. However, there could be significant error in these placements and the interpretation drawn from these.

Anomaly A - This north dipping anomaly, appearing as a arcuate structure in Figure 7 is broadly coincident with the mapped limestone and marble unit, with example of calc-silicate and skarn alteration (samples BDR 3, 21 and 26). The limestone and marble units are described as hematite and limonitic stained, which could be the weathered products of pyrite, accounting for the high chargeability. In addition, pyrrhotite (and other sulphides) are hosted in the calc-silicate and skarn alteration which is consistent with a chargeable response. The resistivity of this chargeable anomaly is variable and there is little correlation with the chargeability. This is consistent with a limestone / marble mapping which can have a wide range of resistivity depending of the extent of fracturing within the sample. There are two VLF anomalies within the chargeable zone. VLF-anomaly g passes immediately north of sample site BDR 26 & 28, which is on the northern edge of a 60 mV/V feature at 325 S on L300 E. VLF-anomaly c is 25 m north of trench T5 and although is offset from the highest chargeability zone on L100 E, is still on a 40 mV/V chargeable zone. The 1999 drilling program did not target the chargeability highs and there are several very high chargeability features, presumably sulphide-rich, calc-silicates or skarns, none of which have been drill-tested, that are good prospects.

Anomaly B - This thin, shallow, chargeable anomaly (50 m) has a strike length of 400 m and is well correlated with the elevated soil geochemistry. It maps within the calc-silicate / skarn unit of the 1999 geology map. On L100 W, the soil anomaly is slightly shifted downslope. Trench T9, with high anomalous gold values, is within this zone. VLF-anomaly b, the most robust VLF feature of the survey runs through the IP anomaly on line 300 W at 25 S and on line 200 W at 75 S. Anomaly B, in contrast to anomaly A, is generally well correlated with low-resistivity. None of the chargeable highs have been drill-tested and as anomaly B is shallow with a soil signature, it is a prospective trenching target.

Anomaly C - This geophysical anomaly has a similar geophysical signature as anomaly B and therefore may be an extension, laterally shifted by the fault at L300W. There are elevated gold soil geochemical values over the anomaly on L400W @ 200 S and L300W at 200S and the trench T12 (with values as high as 2296 ppb) is close-by.

There is also a favourably located VLF anomaly running through it. The northern anomaly has no soil geochemical signature but is modelled as being a deeper body.

Anomaly D - Above the marble-limestone unit is a quartzite unit interbedded with phyllites. The phyllite could be the source of the conductive anomalies on top of the high chargeability zone, seen to the north of anomalies A, B and C.

The drilling program of 1999 had intersections with sulphide mineralization, but as seen in Figure 10, missed the strong chargeable zones. Note the scale is different on Figure 10 with the maximum chargeability being 35 mV/V as compared to Figure 6 and Appendix D with a scale of 0-80 mV/V.

13.0 CONCLUSIONS

- A arcuate zone of elevated chargeability, approximately 300 metres wide, from line 200 W extending 500 m and open to the east, was identified by the IP survey and interpreted to be a calc-silicate, skarn, marble, limestone unit with areas of high sulphide mineralization. This zone is intersected by one NNW VLF anomaly on lines 200 E and 300 E. There are several auriferous calc-silicate and skarn showings within this zone. The areas of high chargeability were not intersected in the 1999 drill program.
- A smaller chargeable zone, coincident with the calc-silicate / skarn unit as previously geologically mapped, correlated well with the elevated Au soil geochemical values. It is thin (10-50 metres), close to the baseline, with a strike length of 400 metres, from line 300 W to 100 E, possibly extended as a more diffuse structure. Samples with anomalous gold values were found within this zone. Although two 1999 holes were drilled close to anomaly B, both missed the areas of highest chargeability.
- Deeper, more modest chargeabilities lie on the western edge of the grid (anomaly C), which may be continuations of anomaly B and present lower priority targets.

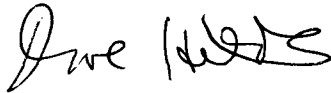
14.0 RECOMMENDATIONS

- Ambiguities in the geographic registration of previous work must be addressed. Prior to any drilling, a survey should be conducted to accurately locate the showings and 1999 drill holes with respect to the 2004 geophysical survey.
- Anomaly A should be further drill tested. The high chargeability zones were

missed in the 1999 drilling program. The targets are (see Figure 6), L200 W @ 200 S; L100 W @ 110 S; L000 E @ 225 S; L000 E @ 275 S; L100 E @ 200 S; L300 E @ 325 S. The last target is coincident with a VLF anomaly.

- Trenching is recommended on anomaly B, either on the highest chargeabilities on L100 W @ 0 N; L000 E @ 50 N or where the strongest VLF anomaly intersects moderate chargeability on L300 W @ 25 S. Another potential intersection between the VLF conductor and the IP anomaly B would be a drill target on L200 W @ 75 S, which was missed by the 1999 hole D99-04.

Respectfully submitted,
AURORA GEOSCIENCES LTD.



Dave Hildes Ph. D.
Geophysicist

REFERENCES

- Davidson, G. S. (1999) Diamond Drill Report on the Dragon Lake Property for Eagle Plains Resources Ltd, Assessment Report.
- Gordey, S. P. and Makepeace, A. J. (1999) Yukon Digital Geology. Geological Survey of Canada, Open File D3826.
- Guilbert, J.M. and Park, C.F. Jr (1986) The Geology of Ore Deposits W.H. Freeman and Company, New York.
- Oldenburg, D.W. and Y. Li (1994) Inversion of induced polarization data. Geophysics Vol. 59. No. 9. pp. 1327-1341.
- Sumner, J.S. (1976) Principles of Induced Polarization for Geophysical Exploration. New York: Elsevier.
- Telford, W.M., L.P. Geldart and R.E. Sheriff (1990) Applied Geophysics (2nd Edition) New York: Cambridge University Press.

APPENDIX A. — CERTIFICATE

I, David Henry Degast Hildes, Ph. D., with residence address in Whitehorse, Yukon Territory do hereby certify that:

1. I am a member in training of the Association of Professional Engineers and Geoscientists of British Columbia.
2. I am a graduate of the Queens University of Ontario with a B.Sc. (Honours) degree in Chemical Physics obtained in 1991 and a graduate of the University of British Columbia with a Ph. D. in Geophysics obtained in 2001.
3. I have been actively involved in mineral exploration since 1999 and am now employed as a geophysicist with Aurora Geosciences Ltd.
4. I conducted the field work described in this report between June 21 and July 11, 2004.

Dated this 21st of DEC, 2004 in Whitehorse, Yukon.

Respectfully submitted,



Dave Hildes, Ph. D

APPENDIX B. — SURVEY LOG

Dragon Lake Survey Log

Dave Hildes (DH)
Warren Kapaniuk (WK)
Anna Crawford (AC)
Qamar Khan (QK)

June 21, 2004 - Mobe

Crew leaves Whitehorse at 1030. Get into Ross River at 1630, the north Canol road closed because of a fire. Talk to forestry and determine that Dragon Lake is in no immediate danger, so continue north. Boat ride is very slow and quit for the night at 0200 with much gear still at truck.

June 22, 2004 - Mobe and Line Cutting

Production: 200 m

WK continues to ferry equipment in morning while AC and QM set up camp. At 0930, DH walks grid and attempting to locate old baseline. Everyone back in camp at 1330 for a line cutting safety meeting, then proceed to start of baseline. WK and QM begin cutting the baseline while DH and AC start line 300E. Back in camp at 1930. Lots of smoke but forestry continues to assure us that we are in no immediate danger.

June 23, 2004 - Line Cutting.

Production: 1300 m

Leave camp at 0830. DH and AC complete cutting and chaining line 300E. WK and QM complete cutting the baseline. Everyone back in camp by 1830. Fire situation is unchanged.

June 24, 2004 - Line Cutting.

Production: 1300 m

Leave camp at 0815. DH and AC cut and chain line 200E. WK and QM cut and chain 000E but saw breaks down 75 m from end of line. Everyone back in camp by 1830. Fire situation is unchanged.

June 25, 2004 - Line Cutting.

Production: 1325 m

Leave camp at 0830. WK and AC finish line 000E and then complete line 100W. Line 100W 50 m short on S end and offset at the north end due to water. DH and QM complete 600 m of line 100E. Back in camp by 1845.

June 26, 2004 - Bear Management, Line Cutting, VLF.

Production: 300 m cut line, 3150 m VLF

Bears came into kitchen during the night to snack on garbage (too dry and too hot to burn anything). They returned at 0730 when 3 bear bangers and a warning shot were fired. Two year old cub returned again and had to be shot. Notified the conservation officer and WK and QM skin bear and dispose of carcass. DH and AC leave at 1045 to begin VLF. WK and QM finish bear duties and begin cutting line 200W at 1400 and are back at camp at 1900. DH and AC back at 1930.

June 27, 2004 - Line Cutting

Production: 1000 m

Leave camp at 0830. DH and AC finish line 100E and 500 m of line 300W. WK and QM complete line 200W and finish chaining the baseline. Realize that the lines have been shifted to the east, so lengthen the baseline spacing on last two wing lines to cover the survey area. Back in camp at 1900.

June 28, 2004 - Line Cutting

Production: 900 m

Leave camp at 0800. DH and QM work on line 300W until DH goes to meet expediter at 1000 for food order. WK and AC cut and chain 400W until chainsaw breakdown at 1700. DH and QM start line 500W. Back in camp by 1815.

June 29, 2004 - Line Cutting, IP

Production: 700 m

Leave camp at 0800. DH and QM work on south end of line 500W, WK and AC complete 400W and north side of 500W. All line cutting done by 1400. The extremely hot and dry weather of the past several weeks is broken by an intense electrical storm. A lightning strike on the other side of lake starts a fire approx 1 km from camp, but luckily heavy rains put the fire out by evening. Spend remainder of day setting up Tx site and running current wire to start of line 300E. Based on the line cutting experience, anticipate radio communication problems for the IP and establish the Tx site on top of hill on the peninsula close to camp. Finish work at 1900.

June 30, 2004 - IP

Production: 800 m

Leave camp at 0830. DH on Rx, AC on Tx, QM on current and WK on cables. Survey line 300E, data quality very good. Move to line 200E and begin survey but have Tx problems at 1630. By 1800, determine that Tx illness is likely terminal and arrange for replacement Tx to leave Whitehorse by late evening.

July 01, 2004 - IP

Production: 900 m

DH leaves to meet truck at 0915, returns by 1100 and helps QM set up Tx. AC (cables) and WK (current) had already left camp to get set up. Complete line 200E and move to 100E. Data quality are quite good. Back to camp by 1920.

July 02, 2004 - IP

Production: 1400 m

Leave camp at 0800. QM on cables, WK on Tx, AC on current and DH on Rx. Complete 100E, 000E and start 100W. Data quality good. Back at camp at 1830. Bear harasses AC during the night.

July 03, 2004 - IP and Demobe

Production: 700 m

Leave camp at 0820. WK on cables, AC on Tx, DH on current and QM on Rx. Complete 100W, begin 200W but have transmitter problems at 1400. Determine that the problem is not field repairable. Clean up all IP gear until 1700 and then begin to demobe camp until just past midnight.

July 04, 2004 - Demobe to Whitehorse

July 05, 2004 - In Whitehorse

July 06, 2004 - In Whitehorse

July 07, 2004 - In Whitehorse

July 08, 2004 - Mobe from Whitehorse

Leave Whitehorse at 0900. Arrive in Ross River to find the Pelly Barge under repair. To everyone's surprise, it is fixed at 1655 and we manage to cross the river before the 1700 closing and establish a camp at the boat launch on Dragon Lake. DH and AC boat out IP gear to grid.

July 09, 2004 - IP

Production: 1100 m

Leave camp at 0745, hour long boat ride to grid. Establish Tx site and continue survey on line 200W. Data is of good quality. Move to 300W where there is a steep outcrop close to baseline (with a showing). Ground is very rocky, data quality becomes quite poor over the outcrop and production is slow. Complete and clean line 300W, then boat back to camp. Back at 2145.

July 10, 2004 - IP

Production: 1400 m

Leave camp at 0730, boat to grid. Survey lines 400W and 500W. Rocky ground results in poor data quality just south of the baseline on 400W. To complete both lines, skip the last few slashes of each line. Begin to pack up IP gear at 1700, back in camp at 1945.

July 11, 2004 - Demobe

Pack up camp and drive south on the North Canol highway to next job.

APPENDIX C. INSTRUMENT SPECIFICATIONS

GEONICS LIMITED
VLF EM 16

Source of Primary Field: VLF transmitting stations

Transmitting Stations Used: Any desired station frequency can be supplied with the instrument in the form of plug-in tuning units. Two tuning units can be plugged in at one time. A switch selects either station.

Operating Frequency Range: About 15-25 Hz

Parameters Measured: (1) The vertical in-phase component (tangent of the tilt angle of the polarization ellipsoid).
(2) The vertical out-of-phase (quadrature) component (the short axis of the polarization ellipsoid compared to the long axis).

Method of Reading: In-phase from a mechanical inclinometer and quadrature from a calibrated dial. Nulling by audio tone.

Scale Range: In-phase $\pm 150\%$; quadrature $\pm 40\%$

Readability: $\pm 1\%$

Reading Time: 10-40 seconds depending on signal strength

Operating Temperature Range: -40 to 50° C.

Operating controls: ON-OFF switch, battery testing push button, station selector, switch, volume control, quadrature, dial $\pm 40\%$, inclinometer dial $\pm 150\%$

Power Supply: 6 size AA (penlight) alkaline cells. Life about 200 hours

Dimensions: 42 x 14 x 9 cm (16 x 5.5 x 3.5 in)

Weight: 1.6 kg (3.5 lbs)

Instrument Supplied With: Monotonic speaker, carrying case, manual of operation, 3 station selector plug-in tuning units (additional frequencies are optional), set of batteries

Shipping Weight: 4.5 kg (10 lbs.)

Name and Address of Manufacturer: Geonics Limited
1745 Meyerside Drive/Unit 8
Mississauga, Ontario
L5T 1C5

6. TECHNICAL SPECIFICATIONS

6.1. MEASURED PARAMETERS

* Time Domain :

- Measurement and display of the voltage, the Self Potential, the IP chargeability (10 fully programmable or preset IP windows), the standard deviation. Display of intensity of current if previously keyed in.

- Continuous stacking of measurements (for noise reduction), display of the number of stacks.

* Frequency Domain

- Measurement and display of the voltage, the self potential, the amplitude of fundamental and of the third harmonic, the frequency effect and phase of the third harmonic with respect to the fundamental, the standard deviations. Display of intensity of current, if previously keyed in.

- Continuous stacking of measurements (for noise reduction), display of the number of cycles (full periods).

* Computation and display of the apparent resistivities and chargeabilities for main electrode arrays : dipole-dipole, pole-dipole, pole-pole, gradient, Schlumberger, Wenner... for 6 dipoles simultaneously.

* Test of dry cells (internal power supply), test of ground resistance of electrodes 1, 3, 4, 5, 6, 7 with respect to 2 (value given between 0.1 kohm and 467 kohm). This test can be manual : RS CHECK function, and this test is also automatic at the beginning of each measurement.

* Test of noise level before the measurements (MONITOR function).

Storage data in the internal memory (up to 2505 readings).

The data which are stored for each reading are :

. In case of TIME DOMAIN :

Station and line numbers, type of electrode array, lengths of lines, voltage, intensity, Self Potential, time parameters, 10 chargeabilities values, standard deviation, the date and time of measurement.

. In case of FREQUENCY DOMAIN :

Station and line numbers, type of electrode array, lengths of lines, voltage, intensity, self potential, the amplitude of fundamental and third harmonic, the frequency effect and phase of the third harmonic with respect to the fundamental, the standard deviations, the date and time of the measurement.

6.2. SPECIFICATIONS

- 6 input channels.
- Input impedance : 10 Mohm.
- Input overvoltage protection up to 1000 Volts.
- Input voltage range - each dipole : 10 V maximum
 - sum of voltages dipoles 2 to 6 : 15 V maximum
- Automatic stacking, automatic SP bucking (-10 V to +10 V).
- 50 to 60 Hz power line rejection
- Common mode rejection : 100 dB (for $R_S = 0$).
- Primary voltage - resolution : 1 μ V after stacking.
 - accuracy typ. 0.3 % ; max 1 over the whole temperature range.
- Battery test : manual and automatic before each measurement.
- Grounding resistance measurement from 0.1 to 467 kohm.
- Memory capacity : 2505 measurements.
- Transfer rates : 300 to 19200 bauds.
- Serial link for data transfer to a printer or a micro computer.
- Remote control of the unit through the serial link (speed : 19200 bauds).

6.2.1. TIME DOMAIN SPECIFICATIONS

- . up to 10 chargeability windows
- . signal waveform : symmetrical time domain (ON +, OFF, ON -, OFF) with a pluse duration (ON TIME) of 0.5, 1, 2, 4 and 8 s.
- . four available I.P. curve sampling choices, three of them are preset times and the fourth one has 10 fully programmable windows.
- . automatic stacking, automatic SP bucking (-10 V to +10 V) with linear drift correction up to 1 mV/s.
- . sampling rate : 10 ms.
- . accuracy in synchronization : 10 ms.
- . minimum voltage for synchronization windows : 40 uV.
- . chargeability - resolution : 0,1 mV/V
 - accuracy typical : 0.6 %, max 2 % of reading ± 1 mV for $V_p > 10$ mV
- . each dipole measurement is stored individually in one memory location.

6.2.2. FREQUENCY DOMAIN SPECIFICATIONS

- . waveform : time domain : ON+, OFF, ON-, OFF
frequency domain : ON+, ON-
- . pulse duration (ON TIME) : 1s, 2s.
- . resolution : about 0.01 degree for unnoisy signals and after stacking.
- . storage in the internal memory : each dipole measurement is stored individually in one memory location.

"ON TIME" (s)	WAVEFORM	NUMBER OF SAMPLES (FFT)	FUNDAMENTAL AND THIRD HARMONIC	
			1	3
0.5	FD	64	1	3
	TD	128	0.5	1.5
1	FD	128	0.5	1.5
	TD	256	0.25	0.75
2	FD	256	0.25	0.75
	TD	512	0.125	0.375
4	FD	512	0.125	0.375
	TD	1024	0.0625	0.1875
8	FD	1024	0.025	0.1875
	TD	2048	0.03125	0.09375

(FD = ON+, ON- ; TD = ON+, OFF, ON-, OFF)

Table of available frequencies (Fundamental and Harmonic).

6.3. GENERAL SPECIFICATIONS

- * Weather proof case
- * Dimensions : length 310 mm, width 210 mm, height 210 mm (12.2 x 8.3 x 8.3 inch)
- * Weight : 5,2 kg (11.5 pounds) without drycells
6 kg (13.2 pounds) with drycells
7,8 kg (17.6 pounds) with the 6 V internal rechargeable batteries
- * Operating temperature : - 20 °C to + 70 °C
(- 40 °C to + 70 °C with an optional screen heater)

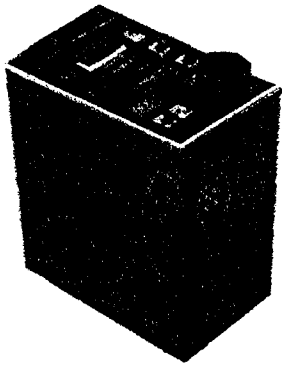
The specifications mentioned on the previous page are given over the entire temperature range.

- * Storage temperature : - 40 °C to + 70 °C with an optimal screen heater.
- * Power supply :

- either : six 1.5 V D size alkaline dry cells or one 12 V external battery
- or : two 6 V internal rechargeable batteries connected in series (=12V) or one 12 V external battery

(The autonomy is 100 hours of operation at 20 °C with a set of new alkaline dry cells and 50 hours of operation at 20 °C with the two charged internal 6V batteries).

Instrumentation GDD



The Induced Polarization Transmitter

TxII-1800 and TxII-3600 Models

For Fast, High-Quality Induced Polarization Surveys in All Field Conditions

Flyers high / low resolution TxII/1 (63 KB) / TxII/2 (1 MB)

At Last, a High-Quality Affordable IP Transmitter

TxII-1800 Model, 1800 watts

Its high power, up to 10 amperes, combined with its light weight and a 21 kg/2000W Honda generator makes it particularly suitable for dipole-dipole Induced Polarization surveys.

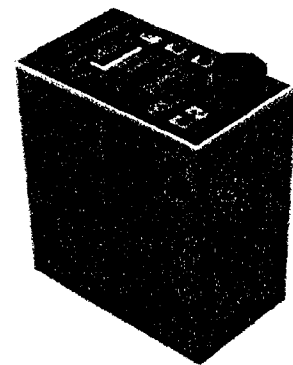
Features

- **Protection against short circuits even at zero (0) ohms**
- **Output voltage range: 150 V to 2400 V / 14 steps**
- **Power source: 120 V, Optional: 220 V / 50/60 Hz**
- **Operates from a light backpackable standard 120 V generator**
- **Up to three years warranty**

This backpackable 1800 watts induced polarization (I.P.) transmitter works from a standard 120 V source and is well adapted to

CONTENTS

- TxII-1800/TxII-3600 IP transmitter**
- Specifications**
- Purchase - Rental**



rocky environments where a high output voltage of up to 2400 V is needed. Moreover, in highly conductive overburden, at 150 V, the highly efficient TxII-1800 watts transmitter is able to send a current of up to 10 amperes. By using this I.P. transmitter, you obtain fast and high-quality I.P. readings even in the most difficult conditions.

TxII-3600 Model, 3600 watts

Its high power, up to 10 amperes, combined with a Honda generator makes it particularly suitable for pole-dipole Induced Polarization surveys.

Features

- **Protection against short circuits even at zero (0) ohms**
- **Output voltage range: 150 V to 2400 V / 14 steps**
- **Power source: 220 V, 50/60 Hz**
- **Operates from a standard 220 V generator**
- **Up to three years warranty**

This 3600 watts induced polarization (I.P.) transmitter works from a standard 220 V source and is well adapted to rocky environments where a high output voltage of up to 2400 V is needed. Moreover, in highly conductive overburden, at 150 V, the highly efficient TxII-3600 watts transmitter is able to send a current of up to 10 amperes. By using this I.P. transmitter, you obtain fast and high-quality I.P. readings even in the most difficult conditions.

Specifications

General		
Size	TxII-1800	21 x 34 x 39 cm
Size	TxII-3600	21 x 34 x 50 cm
Weight	TxII-1800	approx. 20 kg
Weight	TxII-3600	approx. 35 kg

Operating temperature	-40°C to 65°C
Electrical	
Used for time-domain IP	2 sec. ON 2 sec. OFF
Time Base	1-2-4-8 sec.
Output current range	0.005 to 10 A
Output voltage range	150 to 2400 V
Power source TxII-1800	Recommended motor/generator set: Standard 120 V / 60 Hz backpackable Honda generator Suggested Models: EU1000iC, 1000 W, 13.5 kg. or EU2000iC, 2000 W, 21.0 kg.
Power Source TxII-3600	Recommended motor/generator set: Standard 220 V, 50/60 Hz Honda generator Suggested Models: EM3500XK1C, 3500 W, 62 kg or EM5000XK1C, 5000 W, 77 kg
Controls	
Power	ON/OFF
Output voltage range switch	150 V, 180 V, 350 V, 420 V, 500 V, 600 V, 700 V, 840 V, 1000 V, 1200 V, 1400 V, 1680 V, 2000 V, 2400 V
Displays	
Output current LCD	reads to $\pm 0,001$ A
Very cold weather	standard LCD heater on readout
Protection	Total protection against short circuits even at zero (0) ohms
Indicator lamps (in case of overload)	- High voltage ON-OFF - Output overcurrent - Generator over or undervoltage - Overheating - Logic failure - Open loop protection

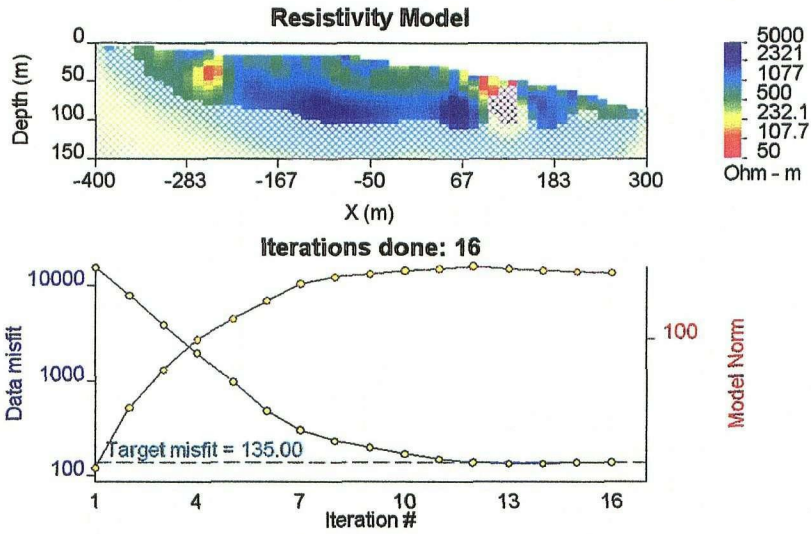
Purchase and Rental Info

Interested by the TxII-1800 W IP or the TxII-3600 W IP transmitter?

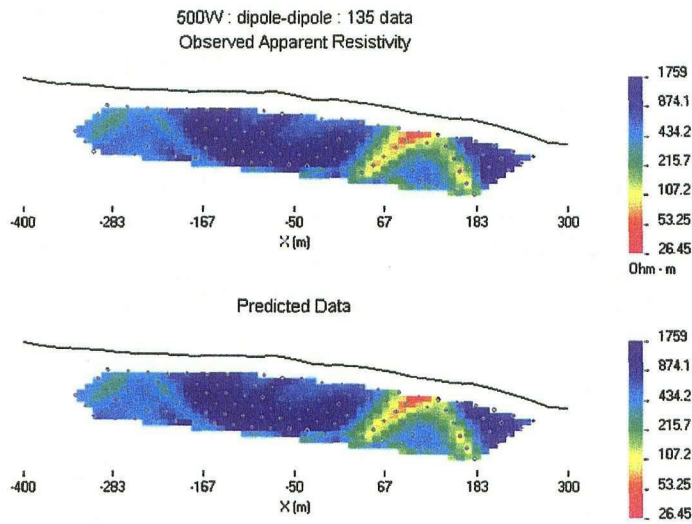
It is simple. You can rent it or purchase it. The choice is yours. Here is some information you

APPENDIX D. INVERSION RESULTS

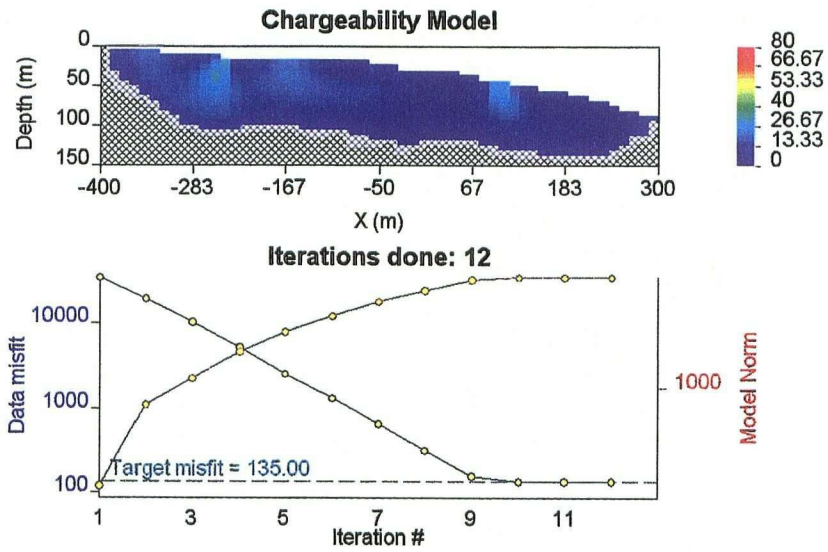
LINE 500 W - Resistivity Model



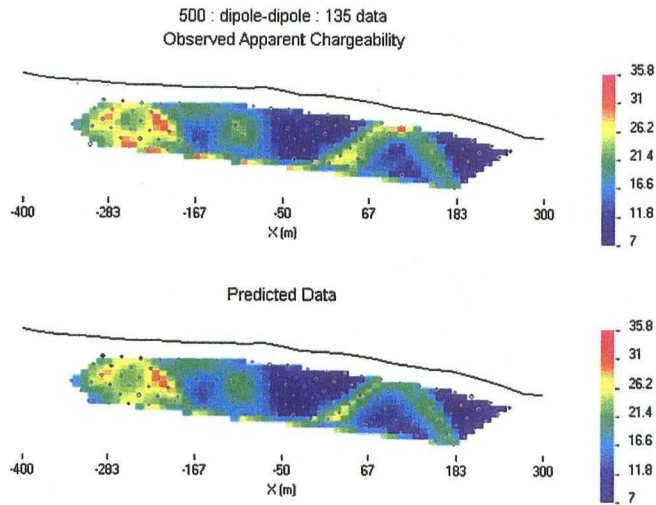
LINE 500 W - Resistivity Pseudosections



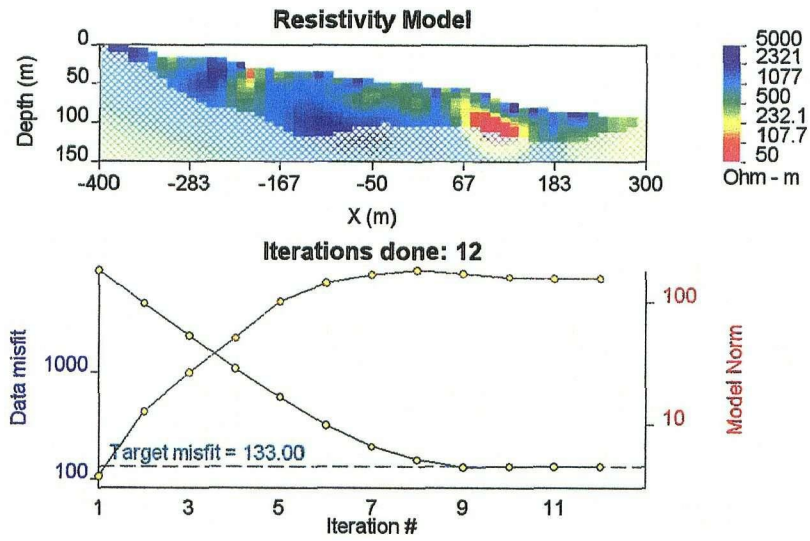
LINE 500 W - Chargeability Model



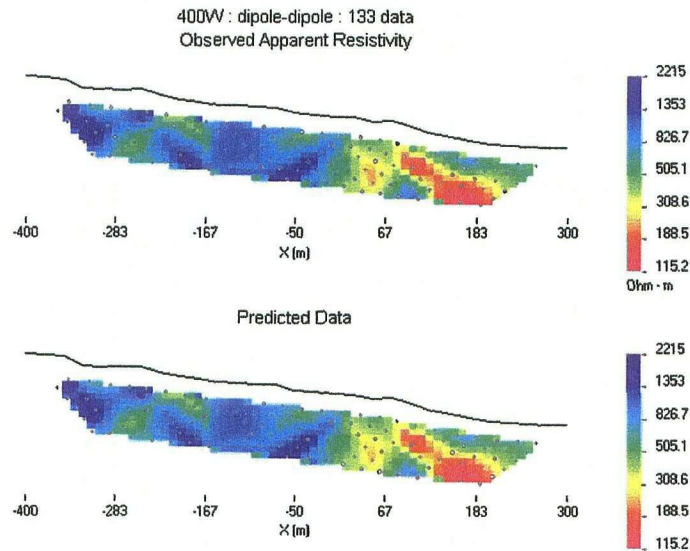
LINE 500 W - Chargeability Pseudosections



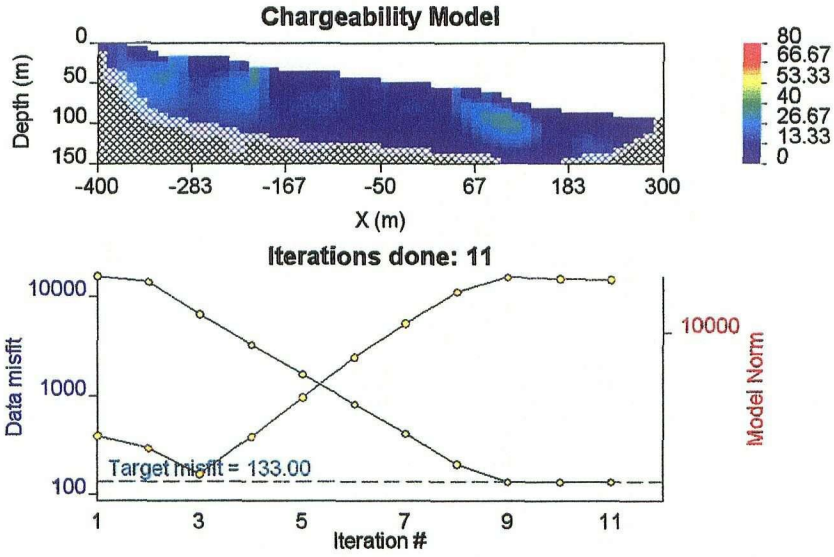
LINE 400 W - Resistivity Model



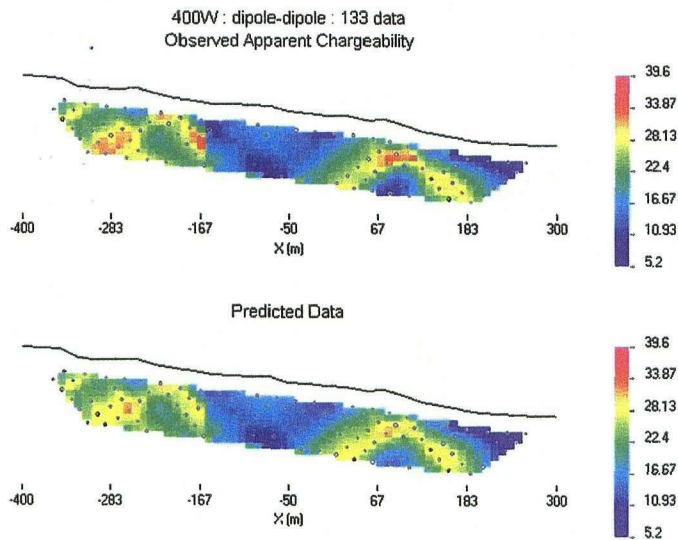
LINE 400 W - Resistivity Pseudosections



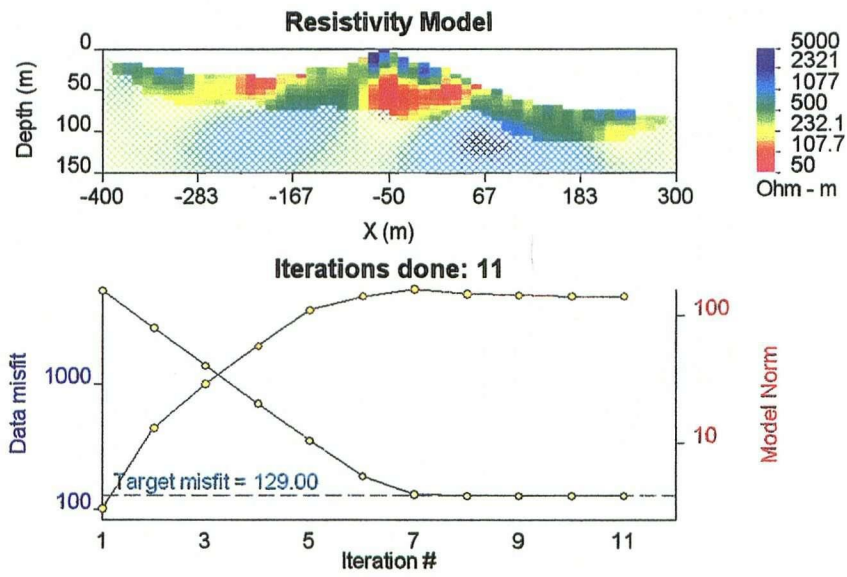
LINE 400 W - Chargeability Model



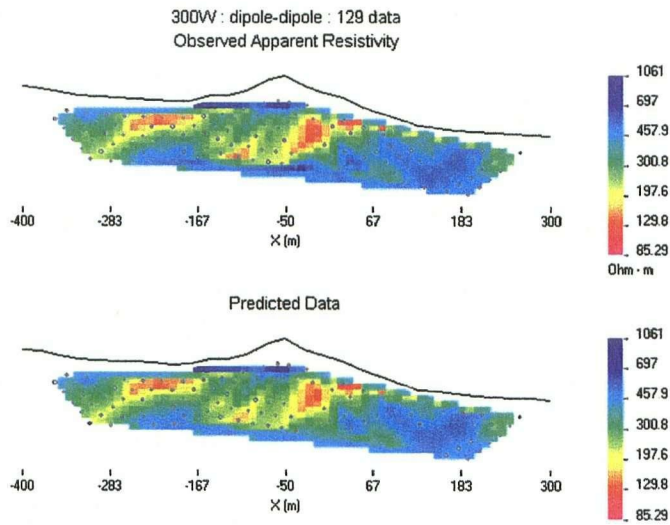
LINE 400 W - Chargeability Pseudosections



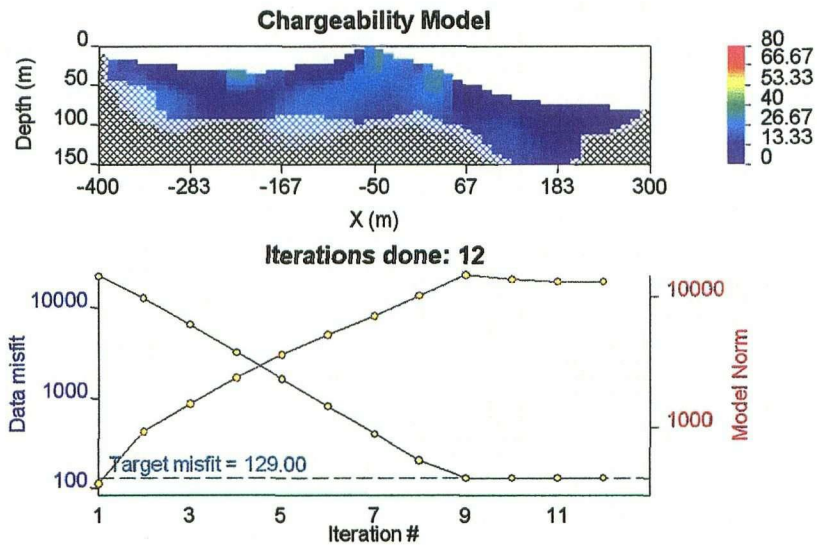
LINE 300 W - Resistivity Model



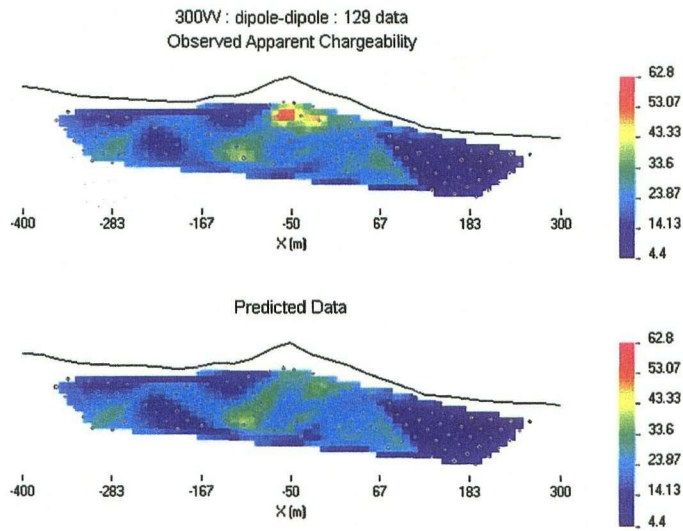
LINE 300 W - Resistivity Pseudosections



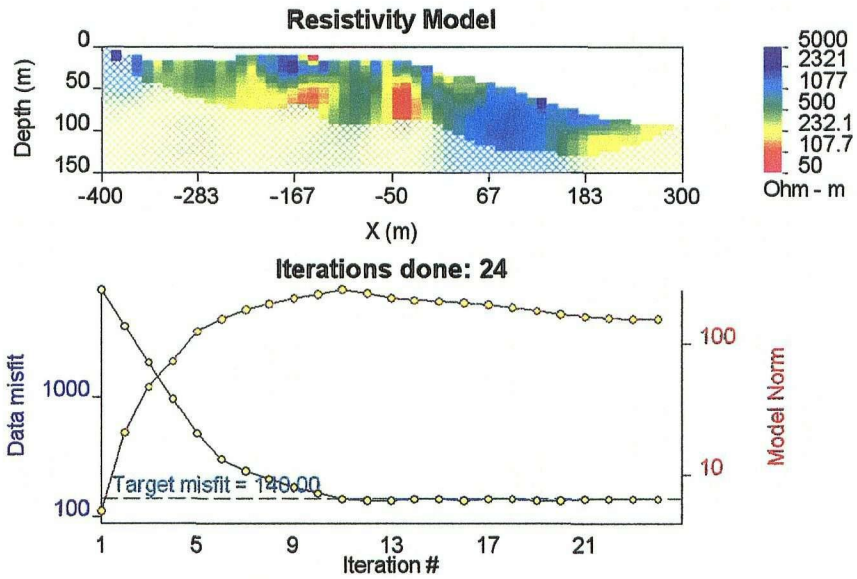
LINE 300 W - Chargeability Model



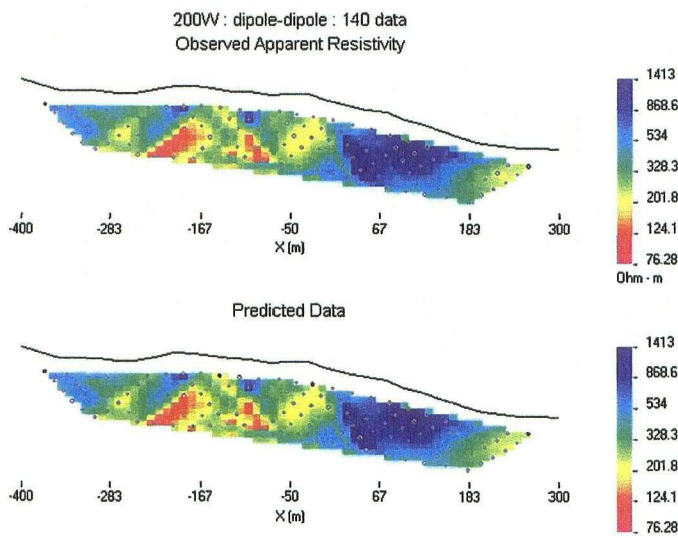
LINE 300 W - Chargeability Pseudosections



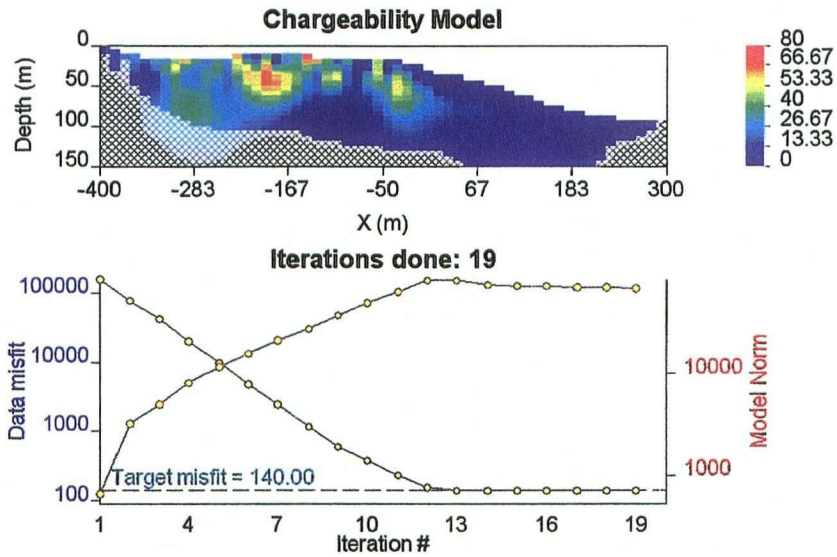
LINE 200 W - Resistivity Model



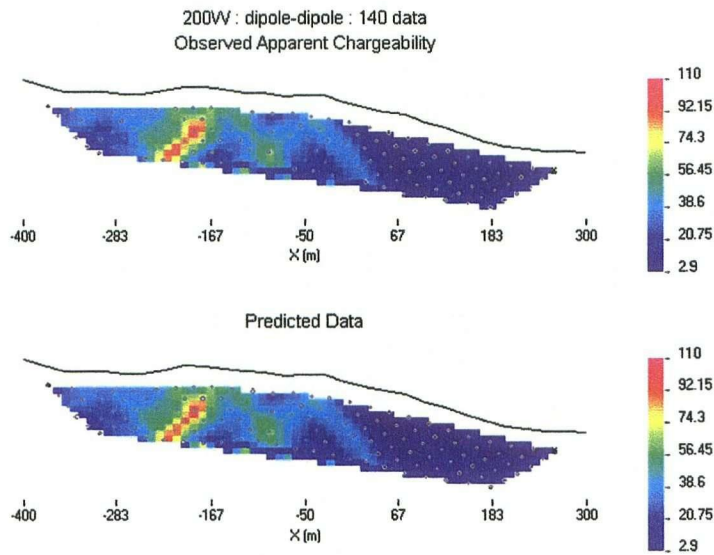
LINE 200 W - Resistivity Pseudosections



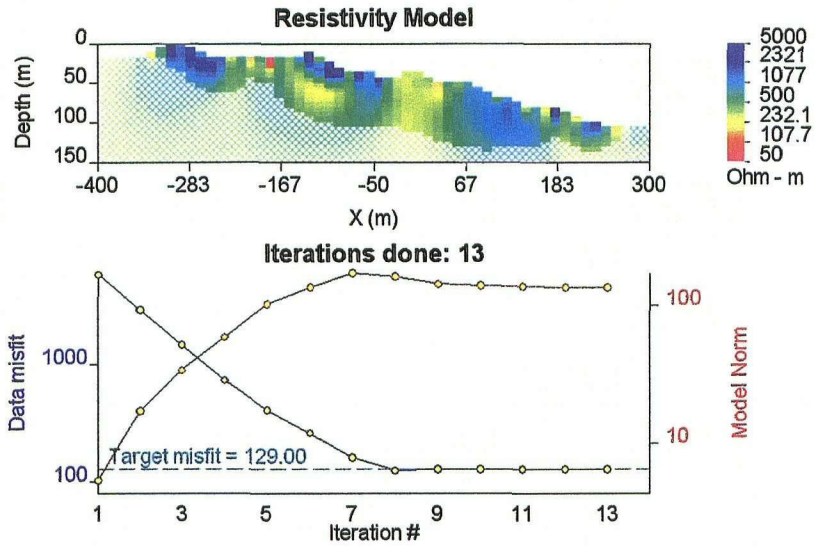
LINE 200 W - Chargeability Model



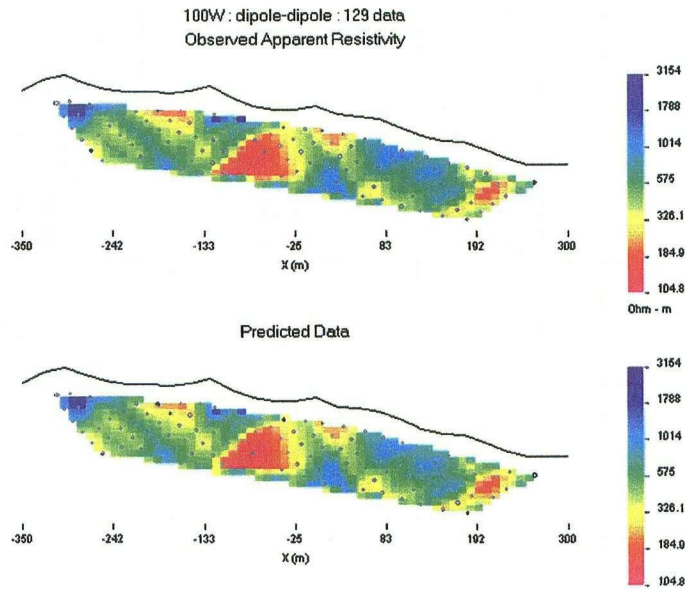
LINE 200 W - Chargeability Pseudosections



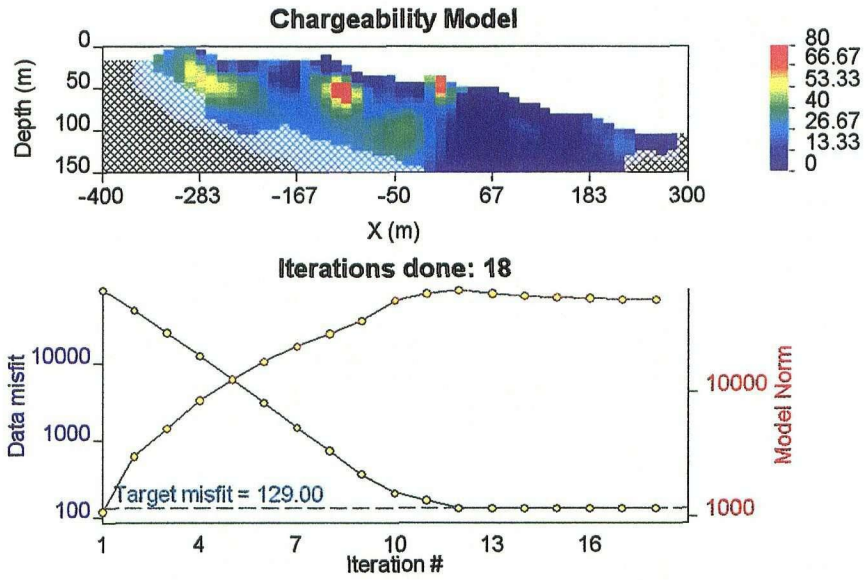
LINE 100 W - Resistivity Model



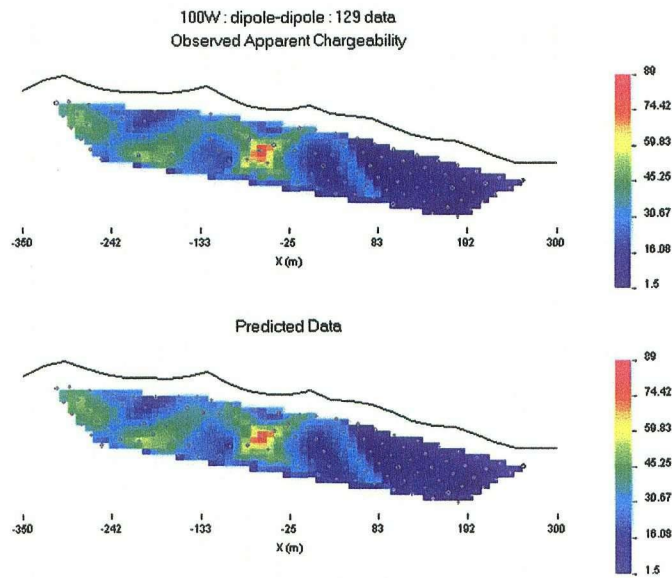
LINE 100 W - Resistivity Pseudosections



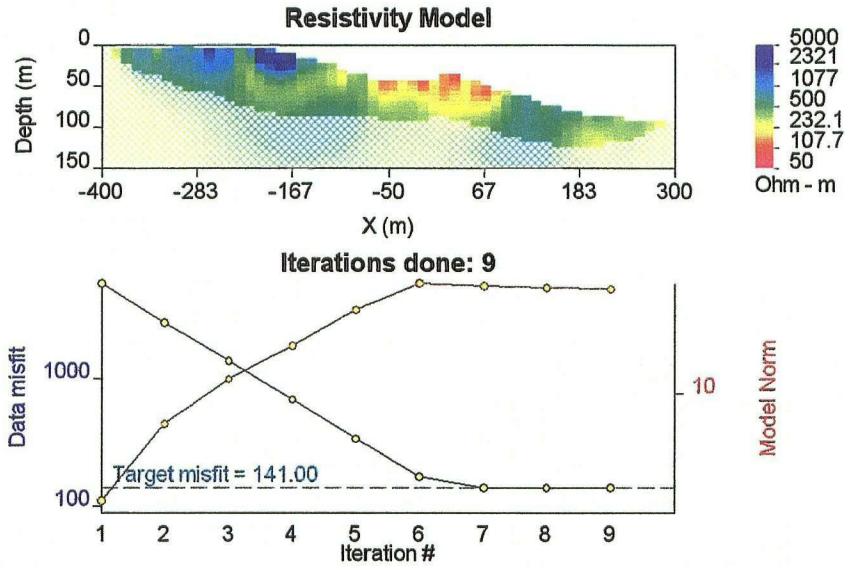
LINE 100 W - Chargeability Model



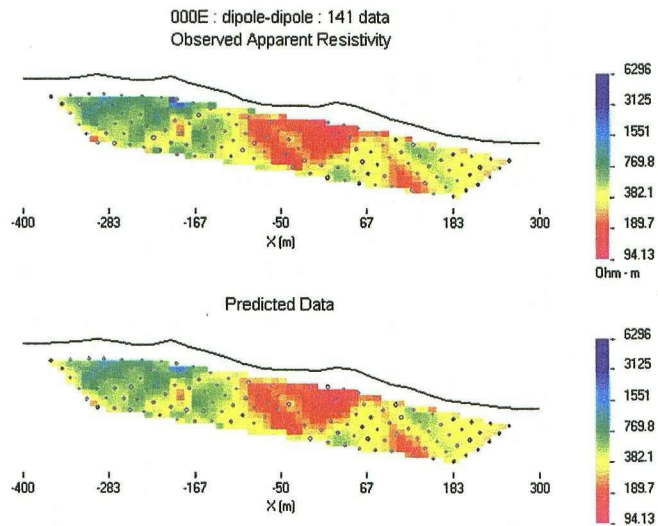
LINE 100 W - Chargeability Pseudosections



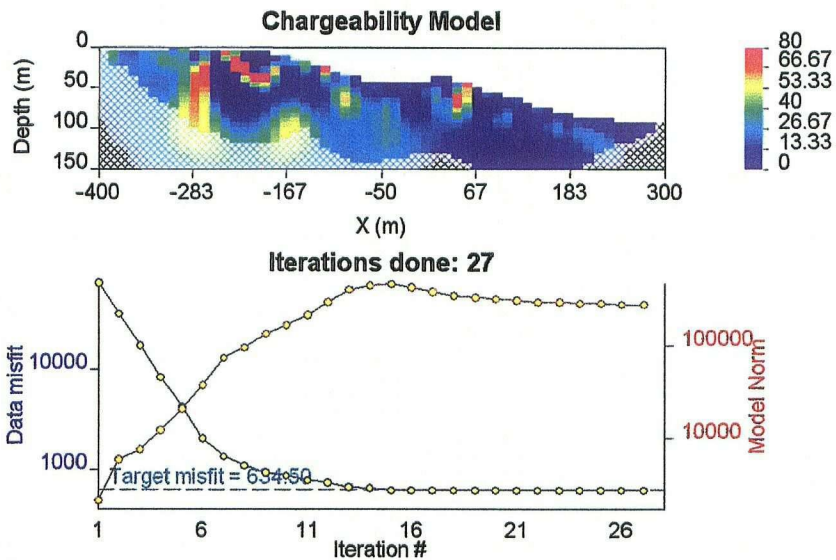
LINE 000 E - Resistivity Model



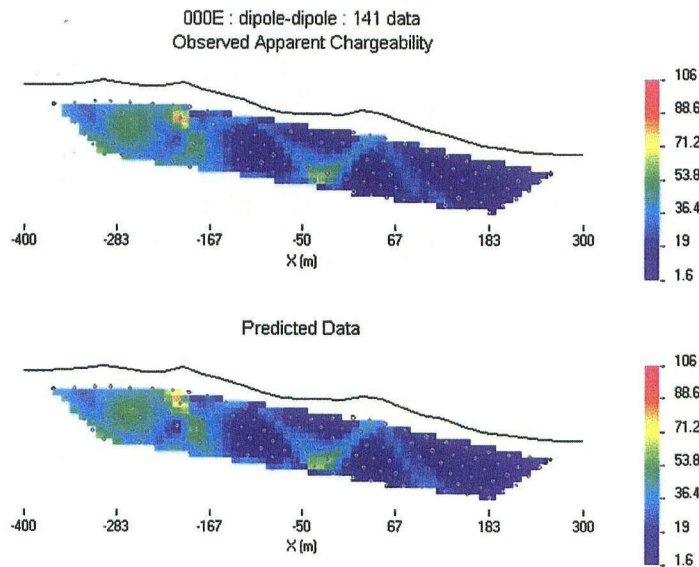
LINE 000 E - Resistivity Pseudosections



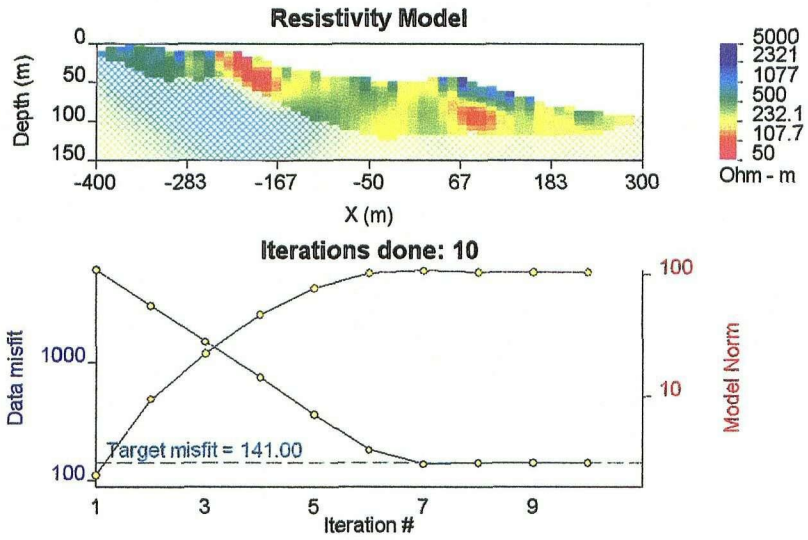
LINE 000 E - Chargeability Model



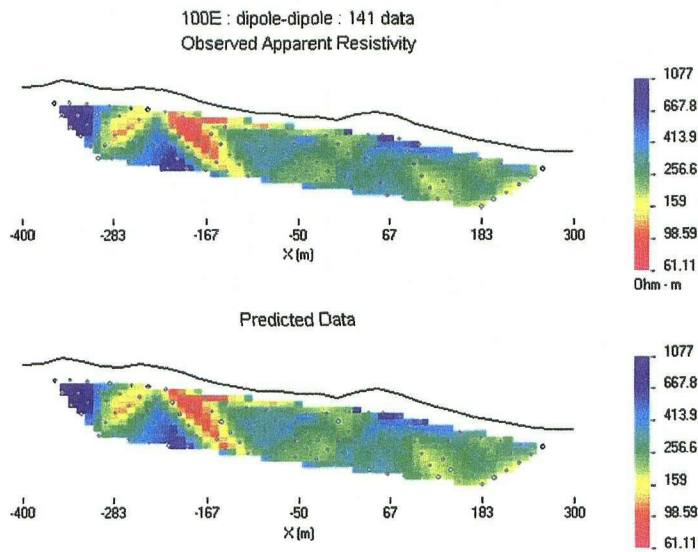
LINE 000 E - Chargeability Pseudosections



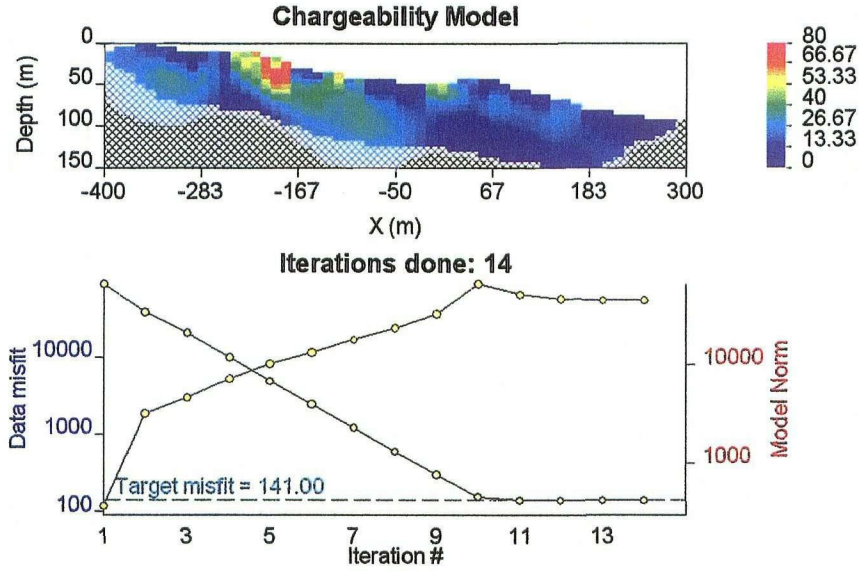
LINE 100 E - Resistivity Model



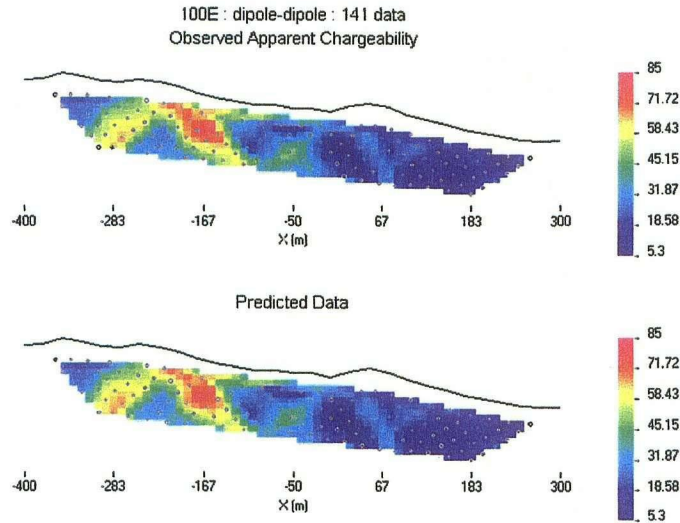
LINE 100 E - Resistivity Pseudosections



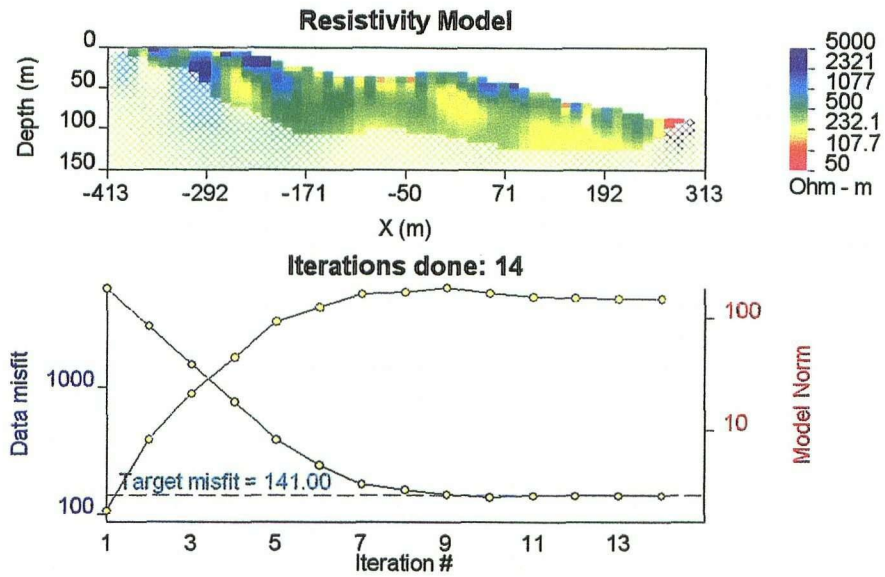
LINE 100 E - Chargeability Model



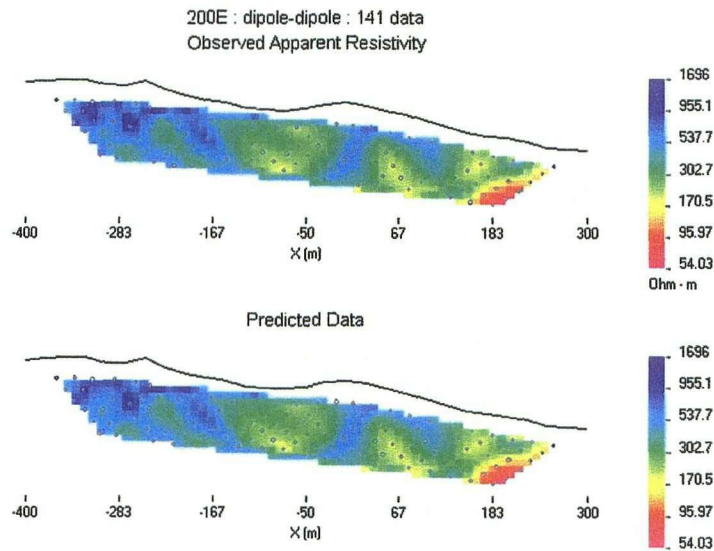
LINE 100 E - Chargeability Pseudosections



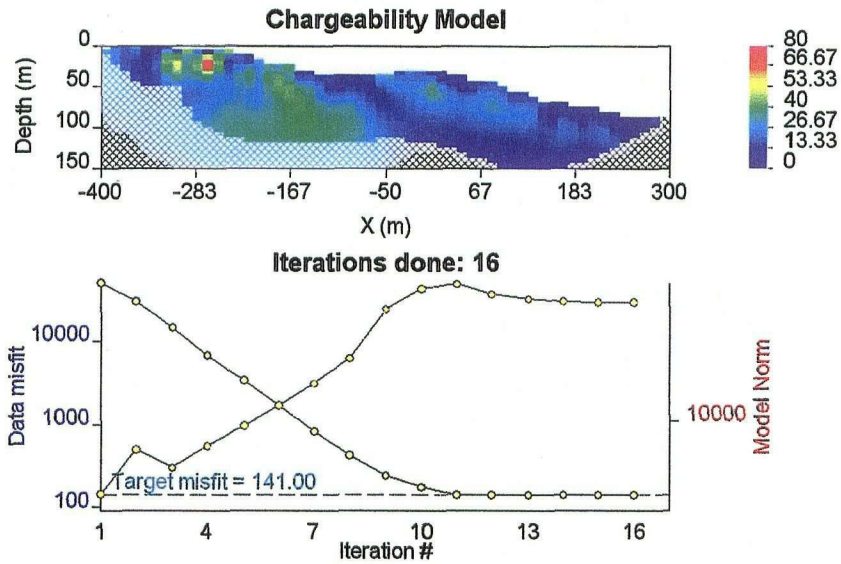
LINE 200 E - Resistivity Model



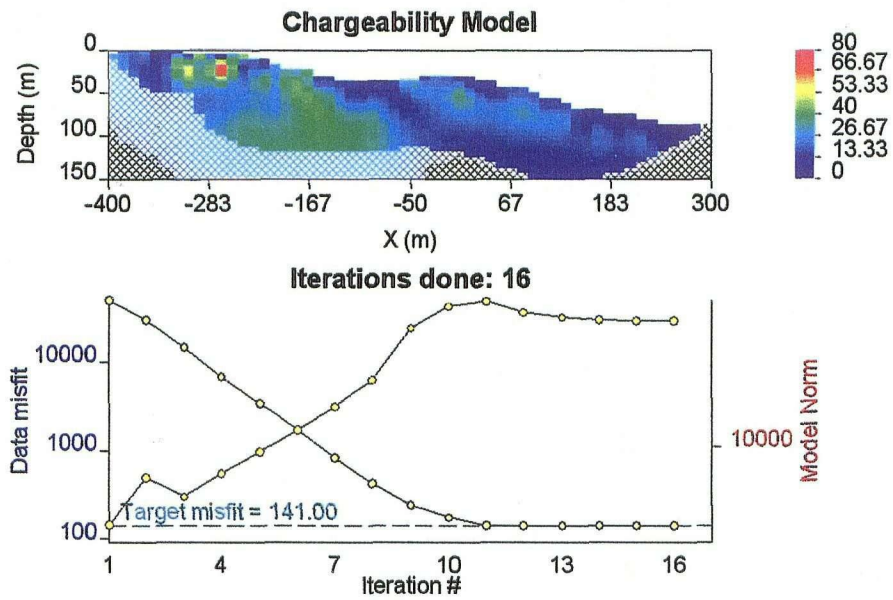
LINE 200 E - Resistivity Pseudosections



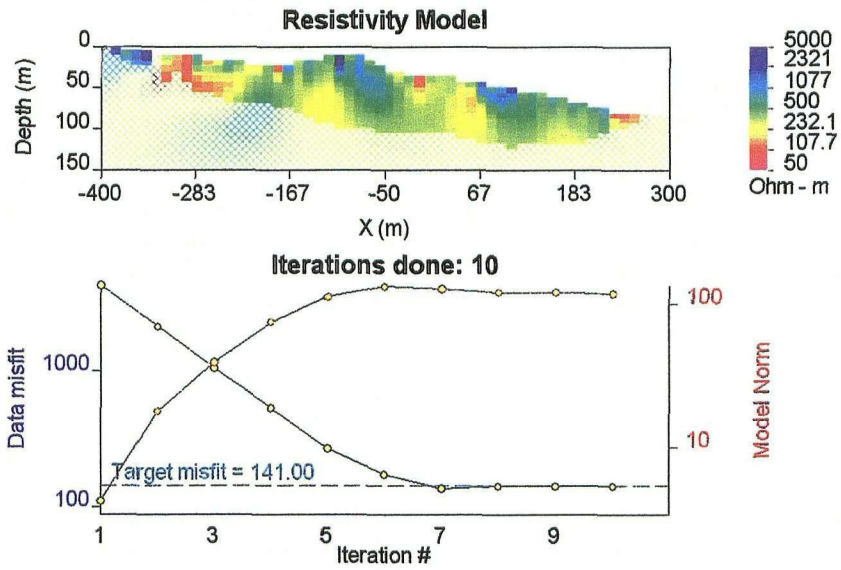
LINE 200 E - Chargeability Model



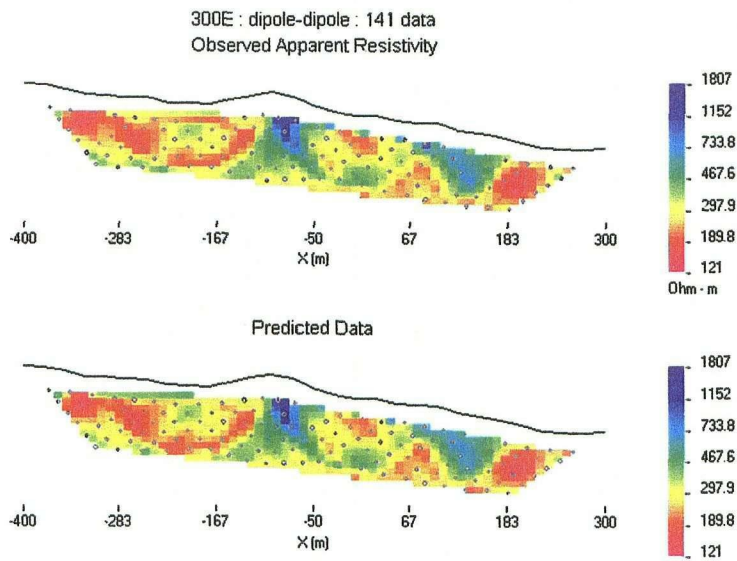
LINE 200 E - Chargeability Pseudosections



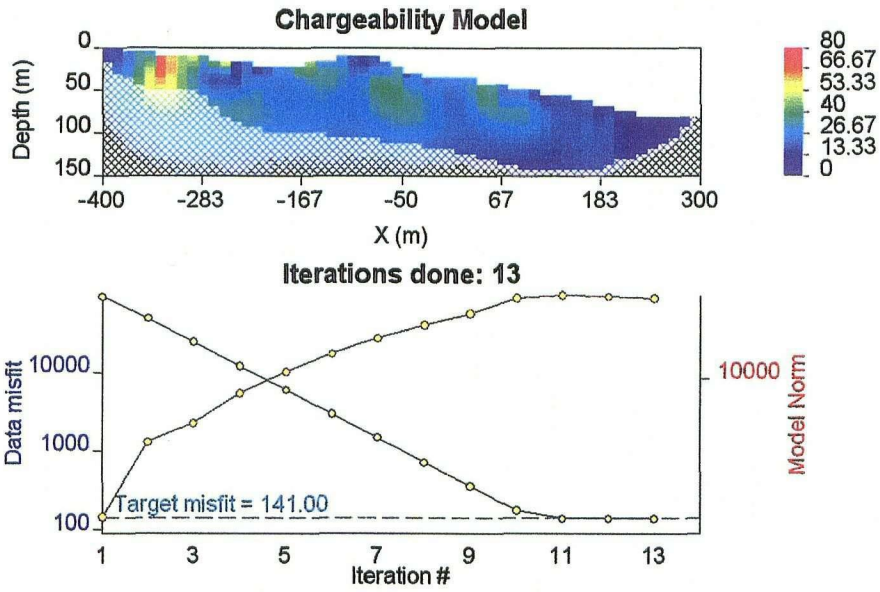
LINE 300 E - Resistivity Model



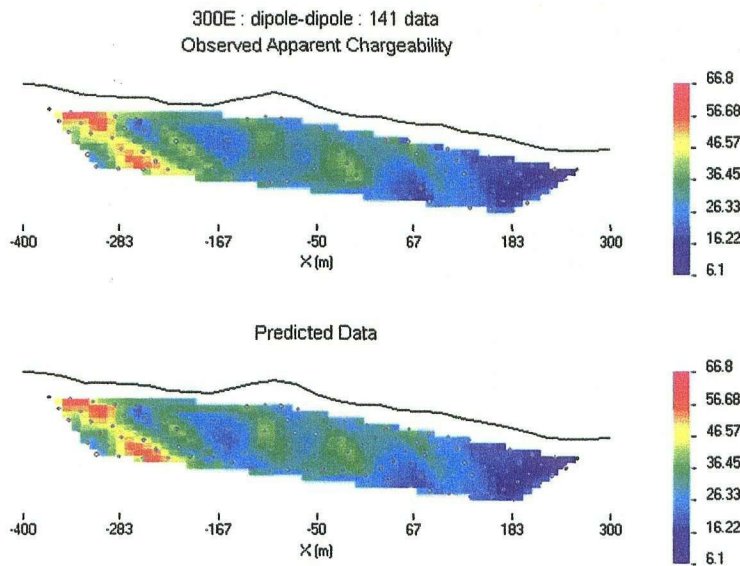
LINE 300 E - Resistivity Pseudosections



LINE 300 E - Chargeability Model



LINE 300 E - Chargeability Pseudosections



APPENDIX F. STATEMENT OF EXPENDITURES (GST included)

Wages (Field Work)		
Dave Hildes	- 8 days @ \$401.25, 6 days @ \$470.80	6034.80
Warren Kapaniuk	- 8 days @ \$342.40, 6 days @ \$401.25	5,146.70
Anna Crawford	- 8 days @ \$342.40, 6 days @ \$321.00	4,665.20
Qamar Khan	- 8 days @ \$342.40, 6 days @ \$321.00	4,665.20
Aurora Geosciences Admin		
		506.42
Geophysical Equipment rental - 6 days @ \$476.15		2,856.9
Linecutting Equipment rental - 8 days @ \$80.25		642.00
Meals		2,333.88
Fuel - gasoline		318.87
Consumables	- flagging, pickets, etc	127.69
Equipment rental	- 14 days @ \$128.40	1,797.60
Vehicle Rental	- 14 days @ \$107.00	1,498.00
Mobilization charges		5,039.70
Maps		71.55
Boat Rental		1,880.95
Report Writing		4,280.00
Total		41,865.46

Yukon Energy, Mines & Resources Library



1000709098

DATE DUE

includes 11 loose maps